

Final Report  
The Resilient Modulus  
of  
Some Connecticut Soils

by

Richard P. Long, Professor  
Jeff E. Crandlemire, Graduate Assistant

JHR 92-216

Project 90-4

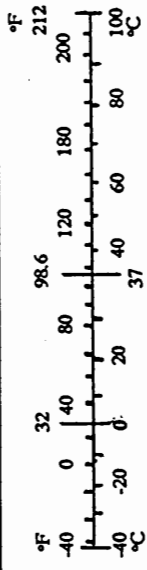
This research was sponsored by the Joint Highway Research Advisory Council (JHRAC) of the University of Connecticut and the Connecticut Department of Transportation and was carried out in the Civil Engineering Department of the University of Connecticut.

The contents of this report reflect the views of the authors, who are responsible for the facts and accuracy of the data presented herein. The contents do not necessarily reflect the official views or policies of the University of Connecticut or the Connecticut Department of Transportation. This report does not constitute a standard, specification, or regulation.

1. Report No. JHR 92-216		2. Government Accession No.		3. Recipient's Catalog No.	
4. Title and Subtitle The Resilient Modulus of Some Connecticut Soils				5. Report Date December 1, 1992	
				6. Performing Organization Code	
7. Author(s) Richard P. Long and Jeff E. Crandlemire				8. Performing Organization Report No. JHR 92-216	
9. Performing Organization Name and Address University of Connecticut Department of Civil Engineering 191 Auditorium Road, Box U-37 TI Storrs, CT 06269				10. Work Unit No. (TRAIS)	
				11. Contract or Grant No.	
12. Sponsoring Agency Name and Address Connecticut Department of Transportation 280 West Street Rocky Hill, CT 06067-0207				13. Type of Report and Period Covered Final Report	
				14. Sponsoring Agency Code	
15. Supplementary Notes					
16. Abstract  The resilient modulus of three Connecticut soils was measured under various conditions of moisture and relative density. The soils were compacted at their optimum moisture content, then tested over a range of water contents while keeping the relative density the same. Relative density was varied by compacting samples dry and wet of optimum. Water content has the more pronounced effect.					
17. Key Words Resilient Modulus, granular soils, gravels			18. Distribution Statement No Restrictions		
19. Security Classif. (of this report) Unclassified		20. Security Classif. (of this page) Unclassified		21. No. of Pages 61	22. Price

# SI\* (MODERN METRIC) CONVERSION FACTORS

APPROXIMATE CONVERSIONS TO SI UNITS				APPROXIMATE CONVERSIONS TO SI UNITS			
Symbol	When You Know	Multiply By	To Find	Symbol	When You Know	Multiply By	To Find
<u>LENGTH</u>				<u>LENGTH</u>			
in	inches	25.4	millimetres	mm	millimetres	0.039	inches
ft	feet	0.305	metres	m	metres	3.28	feet
yd	yards	0.914	metres	m	metres	1.09	yards
mi	miles	1.61	kilometres	km	kilometres	0.621	miles
<u>AREA</u>				<u>AREA</u>			
in <sup>2</sup>	square inches	645.2	millimetres squared	mm <sup>2</sup>	millimetres squared	0.0016	square inches
ft <sup>2</sup>	square feet	0.093	metres squared	m <sup>2</sup>	metres squared	10.764	square feet
yd <sup>2</sup>	square yards	0.836	metres squared	m <sup>2</sup>	hectares	2.47	acres
ac	acres	0.405	hectares	ha	kilometres squared	0.386	square miles
mi <sup>2</sup>	square miles	2.59	kilometres squared	km <sup>2</sup>			
<u>VOLUME</u>				<u>VOLUME</u>			
fl oz	fluid ounces	29.57	millilitres	mL	millilitres	0.034	fluid ounces
gal	gallons	3.785	Litres	L	litres	0.264	gallons
ft <sup>3</sup>	cubic feet	0.028	metres cubed	m <sup>3</sup>	metres cubed	35.315	cubic feet
yd <sup>3</sup>	cubic yards	0.765	metres cubed	m <sup>3</sup>	metres cubed	1.308	cubic yards
NOTE: Volumes greater than 1000 L shall be shown in m <sup>3</sup> .							
<u>MASS</u>				<u>MASS</u>			
oz	ounces	28.35	grams	g	grams	0.035	ounces
lb	pounds	0.454	kilograms	kg	kilograms	2.205	pounds
T	short tons (2000 lb)	0.907	megagrams	Mg	megagrams	1.102	short tons (2000 lb)
<u>TEMPERATURE (exact)</u>				<u>TEMPERATURE (exact)</u>			
°F	Fahrenheit temperature	5(F-32)/9	Celcius temperature	°C	Celcius temperature	1.8C + 32	Fahrenheit temperature



\*SI is the symbol for the International System of Measurement

## Table of Contents

	Page
Title Page . . . . .	i
Technical Report Documentation . . . . .	ii
Metric Conversion . . . . .	iii
Table of Contents . . . . .	iv
List of Figures . . . . .	vi
List of Tables . . . . .	viii
I. INTRODUCTION . . . . .	1
II. BACKGROUND . . . . .	1
A. FATIGUE CRACKING . . . . .	1
B. DEVELOPMENT OF TEST PROCEDURES . . . . .	4
C. DENSITY, MOISTURE, AND OTHER EFFECTS ON THE RESILIENT MODULUS . . . . .	4
III. RESILIENT MODULUS IN FLEXIBLE PAVEMENT DESIGN . . . . .	9
A. RESILIENT MODULUS IN THE BASIC DESIGN EQUATION	10
B. RESILIENT MODULUS IN LAYER CHARACTERIZATION	11
C. LAYER DRAINAGE CHARACTERISTICS . . . . .	13
IV. SCOPE . . . . .	13
V. SAMPLE CLASSIFICATION . . . . .	15
A. GRAIN SIZE DISTRIBUTION . . . . .	15
B. MOISTURE-DENSITY RELATIONS . . . . .	19
VI. TEST EQUIPMENT . . . . .	23
A. SPECIMEN PREPARATION EQUIPMENT . . . . .	23
B. RESILIENT MODULUS TEST EQUIPMENT . . . . .	24
C. EQUIPMENT CALIBRATION . . . . .	27

Table of Contents Cont'd.

1. Load Measurement . . . . .	27
2. Strain Tests Using Synthetic Specimen .	27
VII. SPECIMEN PREPARATION AND TEST PROCEDURE . . . .	29
A. SPECIMEN PREPARATION . . . . .	29
B. TEST PROCEDURE . . . . .	30
VIII. DATA ANALYSIS AND RESULTS . . . . .	32
A. GENERAL . . . . .	32
B. PERCENT SATURATION AND THE RESILIENT MODULUS	33
C. DRAINAGE CONDITIONS AND THE RESILIENT MODULUS	36
D. COMPACTION WATER CONTENT AND THE RESILIENT MODULUS . . . . .	44
IX. SUMMARY AND CONCLUSIONS . . . . .	47
REFERENCES . . . . .	52

## List of Figures

	Page
Figure 1	Load-Deflection Curves for Cracked and Uncracked Pavement Sections . . . . . 3
Figure 2	Resilient Modulus vs. Deviator Stress for a Subgrade Soil (After Wilson, et al) . . . . . 6
Figure 3	Typical Roadway Cross-Section . . . . . 12
Figure 4	GRAIN SIZE DISTRIBUTION OF MONROE SOIL . . . 16
Figure 5	GRAIN SIZE DISTRIBUTION OF WINSTED SOIL . . . 17
Figure 6	GRAIN SIZE DISTRIBUTION OF CONNDOT SOIL . . . 18
Figure 7	MONROE SOIL MOISTURE-DENSITY CURVE . . . . . 20
Figure 8	WINSTED SOIL MOISTURE-DENSITY CURVE . . . . . 21
Figure 9	CONNDOT SOIL MOISTURE-DENSITY CURVE . . . . . 22
Figure 10	Flow Diagram for Instron Model 1331 Operation . . . . . 25
Figure 11	Instron 1331 Schematic . . . . . 26
Figure 12	Resilient Modulus vs. Confining Stress for the Monroe Soil at Various Percent Saturations . . . . . 35
Figure 13	Resilient Modulus vs. Bulk Stress for the Monroe Soil at Various Degrees of Saturation 38
Figure 14	Resilient Modulus vs. Confining Stress for the Monroe Soil in the Drained and Undrained States . . . . . 39
Figure 15	Resilient Modulus vs. Confining Stress for the Monroe Soil in the Drained and Undrained States . . . . . 40
Figure 16	Undrained Resilient Modulus vs. Confining Stress for the Monroe Soil at Various % Saturations . . . . . 41
Figure 17	Resilient Modulus vs. Confining Stress for the Winsted Soil in the Drained and Undrained States . . . . . 42

List of Figures Cont'd

Figure 18	Resilient Modulus vs. Confining Stress for the Winsted Soil in the Drained and Undrained States . . . . .	43
Figure 19	Resilient Modulus vs. Confining Stress for the CONNDOT Soil in the Drained and Undrained States . . . . .	45
Figure 20	Drained vs. Undrained Resilient Moduli for Monroe Soil . . . . .	46
Figure 21	Effect of Varied Compaction Water Contents on the Resilient Modulus of Winsted Soil .	48
Figure 22	Effect of Varied Compaction Water Contents on the Resilient Modulus of CONNDOT Soil .	49

## List of Tables

		Page
Table 1	Resilient Modulus as a Function of Percent Saturation and Bulk Stress (After Rada and Witczak) . . . . .	9
Table 2	Quality of Drainage of Soils - from the Proposed AASHTO Guide for the Design of Pavement Structures . . . . .	13
Table 3	Layer Drainage Characteristics, (m), of Soils - from the Proposed AASHTO Guide for the Design of Pavement Structures . . . . .	14
Table 4	Gradation Characteristics of Soils . . . . .	19
Table 5	Moisture-Density Properties of Soils . . . . .	23
Table 6	Test Sequence for Granular Specimens Base/Subbase Material . . . . .	31
Table 7	Regression Coefficients for Monroe Soil as a Function of Degree of Saturation . . . . .	34
Table 8	Regression Coefficients for Monroe Soil as a Function of Bulk Stress . . . . .	36
Table 9	Regression Coefficients for Drained and Undrained Conditions . . . . .	37
Table 10	Regression Coefficients for Various Compaction Water Contents . . . . .	47



## I. INTRODUCTION

In 1986, the American Association of State Highway and Transportation Officials (AASHTO) adopted a design procedure, based on the elastic behavior of layered media [1]. This procedure is based on a material property called Resilient Modulus ( $M_r$ ). It is a measure of a soil's elastic response to stress as determined by AASHTO Test Method T274-82 [2]. Specifically, the resilient modulus is the ratio of stress to recoverable strain computed using measured vertical strain toward the end of a prescribed number of load repetitions.

The resilient modulus is a function of compaction conditions and subsequent water content at the time of loading. The  $M_r$  varies seasonally with the changes in water content. This variation is provided for in the design procedure through an average value of  $M_r$ . This average value is found by evaluating the  $M_r$  for each fifteen day period throughout the year.

The work reported here investigates the effects of compaction conditions and moisture content during the time of testing for three Connecticut soils. These samples included soils from the towns of Monroe and Winsted as well as a CONNDOT Processed Soil.

## II. BACKGROUND

### A. FATIGUE CRACKING

Research has shown that fatigue cracking of pavement is due to the magnitude of transient deflection from repeated load applications [3].

The 1986 AASHTO design guide specifies the resilient modulus as the property to characterize base, subbase, and subgrade soils for roadway use. The resilient modulus is defined as the ratio of the deviator stress to the resilient, or recoverable, strain:

$$M_r = (\sigma_d) / (\epsilon_r) \quad 1$$

Experimentally, the resilient modulus is determined by measuring the strain recovered from the sample after a prescribed number of load applications. The resilient modulus is normally graphed as a function of either the confining stress or bulk stress:

$$M_r = K1(\sigma_c)^{K2} \quad 2$$

$$M_r = K_1' (\theta)^{K_2'}$$

3

where

$\sigma_c$  = total confining stress

$\theta$  = bulk stress =  $\sigma_1 + \sigma_2 + \sigma_3$

$K_1, K_2$  = regression coefficients using confining stress

$K_1', K_2'$  = regression coefficients using bulk stress

Research indicates that the resilient modulus is dependent on confining stress, degree of saturation, density, and the percentage of fines by weight [4,5,6,7]. In general, the resilient modulus of a soil increases with increasing confining stress, decreasing percent saturation, and increasing density.

A test program was developed at the The University of Connecticut Civil Engineering Department to investigate the effects of various parameters on the resilient modulus of three granular Connecticut soils. Specifically, the effects of drainage conditions and compaction water content were investigated.

In 1955, F.N. Hveem [3] reported the investigation of the fatigue failures of asphalt pavements. These fatigue failures resulted in a pattern of cracking resembling alligator skin or chicken wire patterns.

Hveem reached his conclusions after examining an existing roadway with both cracked and uncracked sections. One section showed fatigue failure in the traffic lane whereas the passing lane was uncracked. He attributed the cracking to a larger number of load applications in the traffic lane as compared to the passing lane. A second section of the roadway showed no signs of fatigue failure in the traffic lane, even though it received the same number of loadings.

Hveem tested the load versus deflection properties of each pavement section. A graph similar to Fig. 1 shows the results of the test. He concluded that the fatigue failure of asphalt pavement is due to the magnitude of the surface deflection and the number of load applications on the pavement, the more important of the two being the amount of deflection.

Hveem also monitored the deflections of the upper eight to nine feet of several pavement systems and noticed a difference in the deflections for uncracked systems which were less than 0.020" and cracked systems which were greater than 0.14". His conclusion was that roads subject to frequent, heavy loads will experience fatigue failure if the deflections

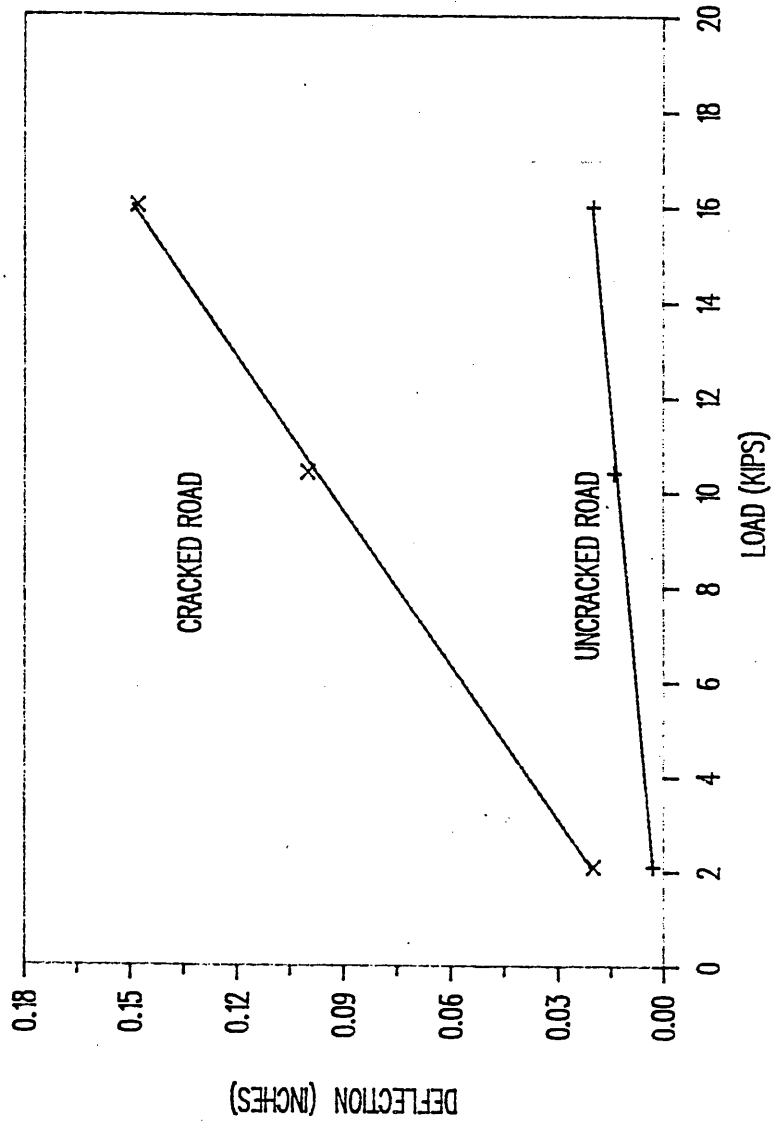


Fig. 1 Load-Deflection Curves for Cracked and Uncracked Pavement Sections

are somewhat greater than 0.020".

In the laboratory, Hveem used his resiliometer, a 1-D dynamic compression apparatus, to measure the deflections of two soils under varied water contents. One sample, an expansive soil, showed increasing deflections with increasing water content. The second soil, a well graded gravel, showed decreasing deflections with increasing water content. He tentatively concluded that, under heavy loads, a marked increase in an expansive soil's deflection may result as the saturation increases.

## B. DEVELOPMENT OF TEST PROCEDURES

With the identification of deflection under transient load as the critical parameter, investigators quickly developed techniques for measuring quasi elastic properties using repetitive loads in a triaxial apparatus. Seed et al, [4] reported some results that showed:

1. A plot of the logarithm of bulk stress against the logarithm of  $M_r$ , as well as the plot of the logarithm of confining stress against the logarithm of  $M_r$  fell along a straight line.
2. An accurate estimate of the stresses in the layers below the pavement is necessary to determine the proper  $M_r$  for design.
3. A greater value for the  $M_r$  of gravel in a saturated, drained condition, than in the dry condition.

AASHTO has developed and refined procedures for testing the resilient modulus of soils used beneath pavements [8]. Although these procedures are general and require that the  $M_r$  be measured over a range of bulk and confining stresses, recommendations have appeared in the literature to focus the testing at the confining stress that represents stress conditions beneath a pavement. The present AASHTO procedures are mute on conditions of sample preparation and the moisture content of the samples tested.

## C. DENSITY, MOISTURE, AND OTHER EFFECTS ON THE RESILIENT MODULUS

Seed, et al, [4] also conducted a limited number of resilient modulus tests on saturated samples of gravel. The tests were conducted in the drained condition and all lateral stresses were considered effective stresses. Comparison of

the resilient moduli for the dry and saturated cases shows a higher Mr for the partially saturated samples.

Experimentally, Elliott and Thornton [5] investigated the effects of confining stress and the number of load cycles on the resilient moduli of fine grained soils. Tests were run at 0, 3, and 6 psi confining stress for samples of various water contents. A trend of increasing resilient modulus with increasing confining stress was observed. In addition, the authors observed that the effect of confining stress decreased with increasing water content.

Wilson, et al [6], investigated the resilient moduli of both granular and fine grained subgrade soils. Specifically, the authors looked at the effects of water content and deviator stress on the resilient modulus of each soil. All tests were conducted at 5 psi confining stress.

Tests were conducted on samples with water contents within +/- four percent of the optimum water content for each soil. The clay and silt-clay soils exhibited a large reduction in the resilient modulus for samples compacted at water contents approximately two percent over the optimum water content. The gravels tested showed a decrease in the resilient moduli with increasing water content, but not to the extent seen in the fine grained samples. These results are in agreement with the research conducted by Rada and Witczak [9]. The authors suggest that each soil type may have a unique value of water content such that samples at or above this water content exhibit a rapid reduction in resilient modulus properties. This threshold water content may be the water content at which repetitive loading generates significant pore pressures.

Wilson, et al, [6] prepared graphs of resilient modulus versus deviator stress to demonstrate the general trend of decreasing resilient modulus with increasing deviator stress. A typical plot is shown in Fig. 2.

All soils tested yielded results which indicated a trend of rapidly decreasing resilient modulus with increasing deviator stress in the range of 0 to 2 psi. The resilient modulus became constant at deviator stresses greater than 2 psi. Wilson, et al, indicated that based on this data, resilient modulus of the subgrade soil cannot be accurately represented by one value, since it increases with increasing depth.

In 1970, R.G. Hicks [7] investigated the influence of various factors on the resilient modulus of granular soils including: the number of load cycles, water content (or percent saturation), density, the amount of fines, and the

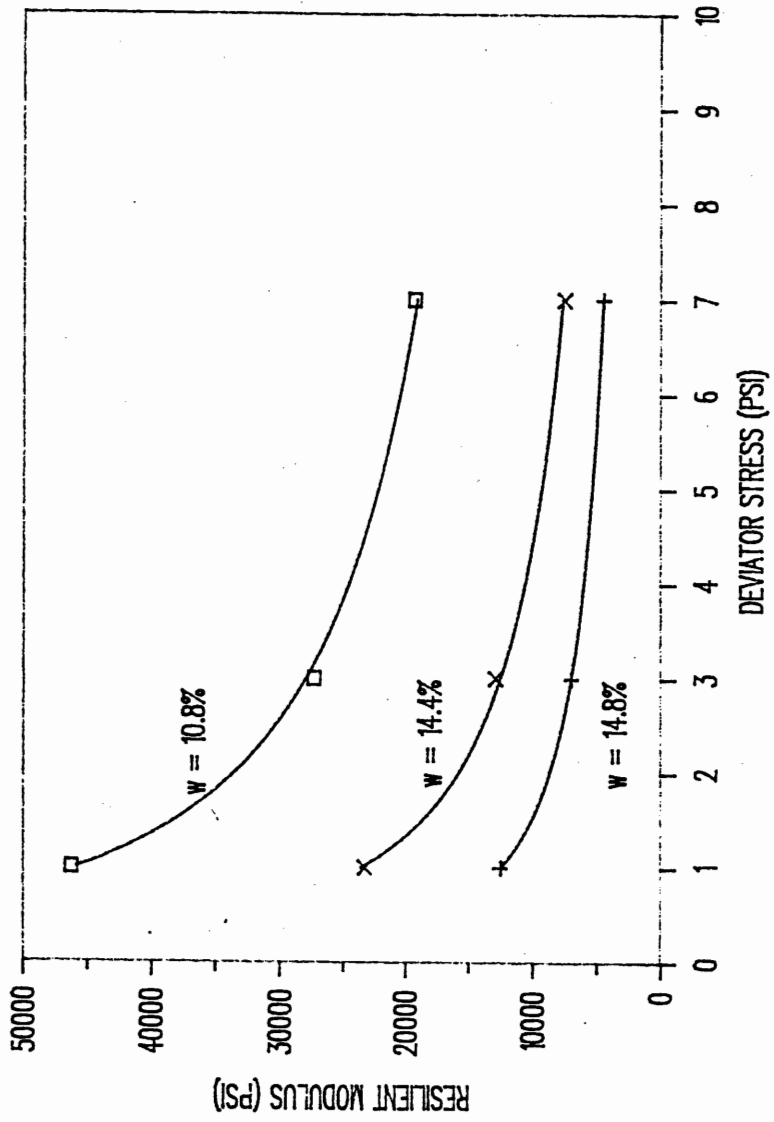


Fig. 2 Resilient Modulus vs. Deviator Stress for a Subgrade Soil  
(After Wilson, et al)

stress level on the resilient moduli of gravels.

Samples were subjected to various numbers of load cycles, some reaching 25,000 load cycles. The resilient modulus of each sample was then measured. Hicks concluded from the data that the resilient modulus determined at 50 or 100 cycles adequately represents the resilient modulus of the soil.

Samples were tested in the dry, partially saturated and saturated states. The author noticed that the resilient modulus of the partially saturated sample was the lowest of the three. Hicks felt that this discrepancy occurred because comparison of the dry and saturated soil was done on the basis of effective stresses, whereas the comparison of the dry and partially saturated samples was done on the basis of total stresses. It is noted in the case of dry samples that the total stress and effective stress are equal. By comparing all samples on the basis of total stresses, a trend of decreasing resilient modulus with increasing water content is observed. These results would indicate that for partially saturated samples, the effective stresses do not necessarily equal the total stresses, and therefore care is needed in evaluating these cases.

Hicks tested samples prepared at various relative densities. He observed a trend of increasing values for the regression coefficients,  $K_1$  and  $K_1'$ , with increasing density. The values of  $K_2$  and  $K_2'$  remained essentially constant. The effect of density on resilient modulus varied from slight to none for the soils tested. Where an effect was noticed, the resilient modulus increased with increasing relative density.

Samples were prepared with soils having 3, 5, and 8 percent passing the number 200 sieve. The author noted that the results of these tests were inconclusive with regards to a relation between the resilient modulus and the amount of fines present. It appeared that the amount of fines altered both the  $K_1$ ,  $K_2$ ,  $K_1'$  and  $K_2'$  values but no general trend was observed. Hicks found that of all factors investigated, the confining stress has the largest effect on the  $M_r$ . The author found considerable increases in the resilient modulus with increasing confining stress, though no quantitative data is listed. The effect of deviator stress was found to have a lesser effect on the resilient modulus than the confining stress. Hicks stated that these results indicate the importance of the stress state in the pavement system in order to properly measure the resilient modulus of each soil.

Rada and Witczak [9] conducted an evaluation of a large database of information on the resilient moduli of granular materials. The information was gathered from other researchers and from tests conducted by the authors.

From a graph of K1 versus K2 for all samples, the authors noticed a trend of decreasing K1 with increasing K2. The data was divided into six categories based on a qualitative analysis of each soil. Each group showed a definite K1-K2 relationship. Large ranges of K1 and K2 values were observed for each class. The authors made the point that these results indicate that each soil must be tested to get an accurate measure of the resilient modulus of that soil. Assuming K1 and K2 values of a typical soil similar to the one in question can lead to errors in the design process.

The authors also determined that percent saturation and density affect the resilient moduli of granular soils. All the data indicated that an increase in saturation caused a decrease in K1 and the resilient modulus. The authors noted that the effect of saturation was different for each soil, and therefore each soil should be tested to determine the exact trend. Although smaller than those associated with changes in percent saturation, a trend of increasing resilient modulus with increasing density was observed.

The authors concluded that the state of stress, relative density of the sample, and percent saturation all significantly affect the resilient modulus of a given soil. A predictive equation for Mr was developed because Eqs. 2 and 3 do not account for the percent saturation and relative density. The equation is of the form:

$$\log(Mr) = C_0 + C_1 \cdot Sr + C_2(PC) + C_3 \log(\theta) \quad 4$$

where

Sr = percent saturation  
PC = percent relative density  
 $\theta$  = bulk stress  
C0, C1, C2, C3 = regression coefficients

The values, shown in Table 1, have been determined for the resilient modulus of a bank run soil using Eq. 4. This analysis investigates the effects of bulk stress and percent saturation on the resilient modulus.

In contrast to Eq. 3, this analysis demonstrates that Eq. 4 is highly sensitive to percent saturation but relatively insensitive to bulk stress. For a bank run gravel at 100% saturation, the resilient modulus varies from 31,500 psi at a bulk stress of 100 psi to 13,500 psi at a bulk stress of 30 psi.



PERCENT SATURATION			
BULK STRESS	100%	50%	0%
100 psi	11340	24901	54680
50 psi	11300	24812	54484
30 psi	11270	24747	54340

Table 1 Resilient Modulus as a Function of Percent Saturation and Bulk Stress (After Rada and Witczak)

The state of knowledge for the resilient behavior of soils leads to the following conclusions:

1. Fatigue cracking in pavements is a function of the number of load applications and the magnitude of the deflections.
2. The resilient modulus test can be used to determine the resilient response of soils, provided careful attention is paid to the factors which influence Mr.
3. Research conducted by various authors indicates that the resilient modulus behavior is influenced by percent saturation, deviator stress, and sample density.

In general, the resilient modulus increases with increasing confining stress and density, and decreasing percent saturation and deviator stress.

### III. RESILIENT MODULUS IN FLEXIBLE PAVEMENT DESIGN

The 1986 AASHTO Guide for Design of Pavement Structures [10] expands upon its predecessor, the "Interim Guide for the Design of Pavement Structures". One of the most important additions to the 1986 edition is the use of the resilient modulus test to determine both the soil support characteristics of the subgrade soil and the pavement layer coefficients for the base and subbase soils. Other considerations given to roadway design are the effects of environmental fluctuations, such as precipitation and temperature, on subgrade soil behavior, and the use of coefficients to quantify the drainage characteristics of the pavement layers.

## A. RESILIENT MODULUS IN THE BASIC DESIGN EQUATION

The resilient modulus is specified as the method of classification by which the support quality of the subgrade soil is determined. Developed by AASHTO, Eq. 5 determines the pavement strength necessary for a given subgrade through the structural number from the equation:

$$\log W_{18} = 9.36 \log(SN+1) - 0.2 + 2.32 \log(M_r) - 8.07 + \frac{[\log((\delta PSI)/2.7)]}{[0.4 + 1094/(SN+1)^{5.19}]}$$
 5

where:

- $W_{18}$  = the number of equivalent 18 kip single axle load applications  
 $M_r$  = resilient modulus of the roadbed soil  
 $\delta PSI$  = pavement serviceability loss from the time of construction to the point where rehabilitation is necessary  
 $SN$  = structural number which represents the required pavement design strength

The structural number is a parameter which indicates the required strength of the cross-section for the given subgrade soil. The structural number and the design of the roadway will be discussed in the next section.

The resilient modulus was selected as the test for the following reasons:

- (1) AASHTO has a test procedure developed for the resilient modulus.
- (2) The resilient modulus is recognized internationally as a classification method for roadway materials.
- (3) The resilient modulus is useful in predicting fatigue cracking in pavements.
- (4) Correlations exist between the resilient modulus and other measured properties such as the California Bearing Ratio.

The resilient modulus is a function of, among other things, water content. The seasonal variations in water content of a soil throughout the year may have a significant impact on the resilient modulus of the soil. AASHTO has developed a method to deal with this problem. The resilient modulus of a particular soil is calculated for calendar divisions of fifteen days. Each fifteen day block is evaluated for the percent saturation expected at the site.

The resilient moduli for all the divisions of the year are summed and divided by the number of divisions. The result is the value,  $M_r$ , used in Eq. 5.

#### B. RESILIENT MODULUS IN LAYER CHARACTERIZATION

The equation given by AASHTO for the design of a layered flexible pavement structure is:

$$SN = a_1 D_1 + a_2 D_2 m_2 + a_3 D_3 m_3 \quad 6$$

where:

$a_i$  = layer coefficient  
 $D_i$  = layer thickness  
 $m_i$  = layer drainage coefficients  
1, 2, 3 represent the surface, base, and subbase courses, respectively.

A cross-section of a typical layered pavement section is shown in Figure 3.

The layer coefficients for the base and subbase soils are determined based on their resilient moduli. The equations relating these two parameters are:

$$\text{Base } a_2 = 0.249(\log M_r \text{ base}) - 0.977 \quad 7$$

$$\text{Subbase } a_3 = 0.227(\log M_r \text{ subbase}) - 0.839 \quad 8$$

The layer coefficients are indicative of the ability of the materials used in a pavement. Inspection of Eqs. 6, 7, and 8 shows that the higher the resilient modulus of a soil, the smaller the required thickness for a given structural number.

Inspection of Eq. 6 illustrates that all layers are represented. The structural number quantifies the strength characteristics of the subgrade soil. The right side of the equation represents the strengths of the asphalt, base, and subbase layers. Thus, Eq. 6 can be viewed as the relation which ties together the strength requirements of the various elements of the pavement.

A second aspect of Eq. 6 is that there is an infinite number of combinations of asphalt, base, and subbase layers which will satisfy the relation for a given structural number. Secondary considerations, such as availability of materials and cost can then be used to determine the most cost effective cross-section for a roadway.

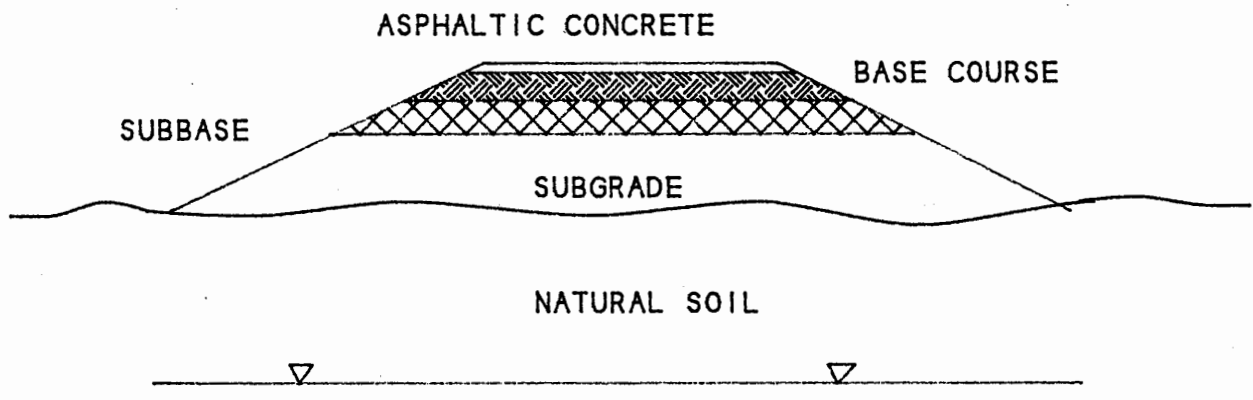


Figure 3 Typical Roadway Cross-Section

### C. LAYER DRAINAGE CHARACTERISTICS

AASHTO treats the topic of layer drainage in very general terms. The AASHTO method is to classify the drainage characteristics of a material based on the amount of time required for water to be removed from the soil (see Table 2). However, the hydraulic gradient by which these classifications are to be determined is not given. No specifics are discussed concerning various drainage schemes.

QUALITY OF DRAINAGE	WATER REMOVED WITHIN
EXCELLENT	2 HOURS
GOOD	1 DAY
FAIR	1 WEEK
POOR	1 MONTH
VERY POOR	WATER WILL NOT DRAIN

Table 2 Quality of Drainage of Soils - from the Proposed AASHTO Guide for the Design of Pavement Structures

AASHTO has incorporated the drainage characteristics of each layer into Eq. 6. The "m" values proposed by AASHTO are listed in Table 3.

### IV. SCOPE

The literature concerning the resilient modulus of granular base materials indicates that water content (or percent saturation) has the greatest effect on the resilient modulus. To understand the resilient behavior of a given soil, it is necessary to determine the effects of moisture on the resilient modulus.

In general, the resilient moduli of in-situ soils fluctuate throughout the year. This is due to varied moisture conditions during each season. The worst case (i.e. lowest resilient modulus) occurs during the spring thaw, when the moisture content is high. This program has investigated the resilient moduli of three Connecticut soils under moisture conditions intended to represent those found during the spring thaw. The goal is to determine quantitative expressions for

QUALITY OF DRAINAGE	PERCENT OF TIME PAVEMENT IS EXPOSED TO MOISTURE LEVELS APPROACHING SATURATION			
	< 1%	1%-5%	5%-25%	>25%
EXCELLENT	1.40-1.35	1.35-1.30	1.30-1.20	1.20
GOOD	1.35-1.25	1.25-1.15	1.15-1.00	1.00
FAIR	1.25-1.15	1.15-1.05	1.00-0.80	0.80
POOR	1.15-1.05	1.05-0.80	0.80-0.60	0.60
VERY POOR	1.05-0.95	0.95-0.75	0.75-0.40	0.40

Table 3 Layer Drainage Characteristics, (m), of Soils - from the Proposed AASHTO Guide for the Design of Pavement Structures

the resilient moduli of the soils. This information is ultimately intended for use in the AASHTO design procedure.

A second topic of investigation is the effect of drainage conditions on the resilient moduli of the three soils. The AASHTO design procedure [10] treats the topic of pavement drainage in a rather vague manner. For this reason, this program investigates the effect of different drainage schemes on the resilient characteristics of each soil.

There are several ways to approach the effect of water content on the resilient modulus. The water content of the soil during compaction affects the dry density obtained for a given compactive effort. In addition the water present during the load application may lower the resilient modulus for a given dry density.

Both of these approaches have been used in the work reported here. When the soil samples are compacted wet and dry of the optimum water content, the effect of dry density is measured and the importance of controlling field compaction is determined. When all the samples are compacted at optimum water content, and the water content is subsequently adjusted before measuring  $M_r$ , the possible seasonal variations of the resilient moduli are obtained. These two methods of reaching a water content allows the designer to estimate  $M_r$  under a variety of conditions.

## V. SAMPLE CLASSIFICATION

Three soils indigenous to Connecticut were tested to determine their resilient modulus characteristics. The samples were provided by the Connecticut Department of Transportation. Two of the soils were collected from borrow pits located in Monroe and Winsted. The third sample was designated as a CONNDOT Processed Soil.

The Monroe soil was a light brown, subrounded, gravelly sand with some fines. The Winsted soil was a dark brown, rounded to subrounded, gravelly sand with a small amount of fines. The particles were rounded to subrounded in shape. The CONNDOT Processed Soil is a dark gray gravel and coarse sand mixture with angular particles.

Several index property tests were performed in order to determine the gradation and moisture-density characteristics of each soil.

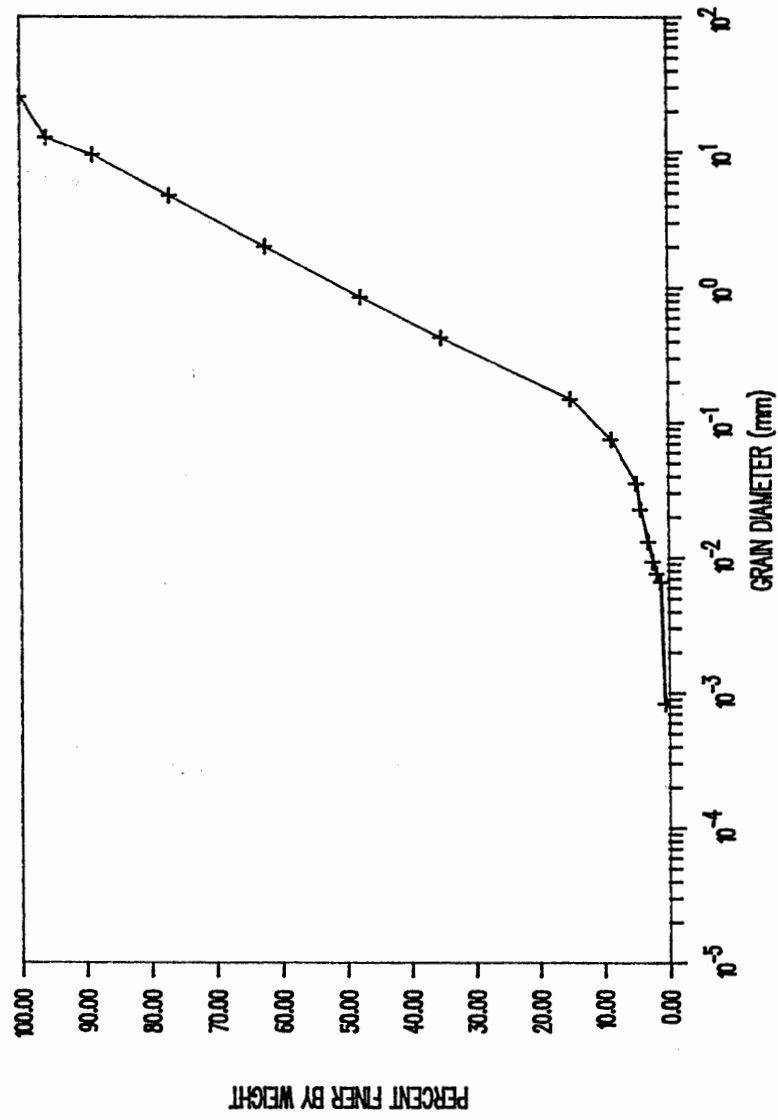
### A. GRAIN SIZE DISTRIBUTION

A sieve analysis was performed on a sample of each soil after being washed of fines on the #200 sieve. A hydrometer analysis was also performed on a representative sample of each soil passing the #10 sieve. Each test was performed in accordance with ASTM Standard D422-63 Standard Method for Particle Size Analysis of Soils.

Grain size distribution curves were prepared for each soil as shown in Figures 4, 5, 6. Each soil was classified using the USCS and AASHTO classification methods as shown in Table 4. The Monroe and Winsted soils are uniform, whereas the CONNDOT soil is well graded. All of the soils are sands with appreciable amounts of fines.

Atterberg limit tests were conducted on sample portions passing the #40 sieve for each soil type in accordance with ASTM Standard D4318-84 Standard Test Method for Liquid Limit, Plastic Limit and Plasticity Index of Soils. The tests indicated that all soils contained non-plastic fines. The results are listed in Table 4:

The soil classifications were used to determine the appropriate test procedure for each soil. This aspect will be further discussed in Section VII, SAMPLE PREPARATION AND TEST PROCEDURE.



GRAIN SIZE DISTRIBUTION OF MONROE SOIL

Fig. 4



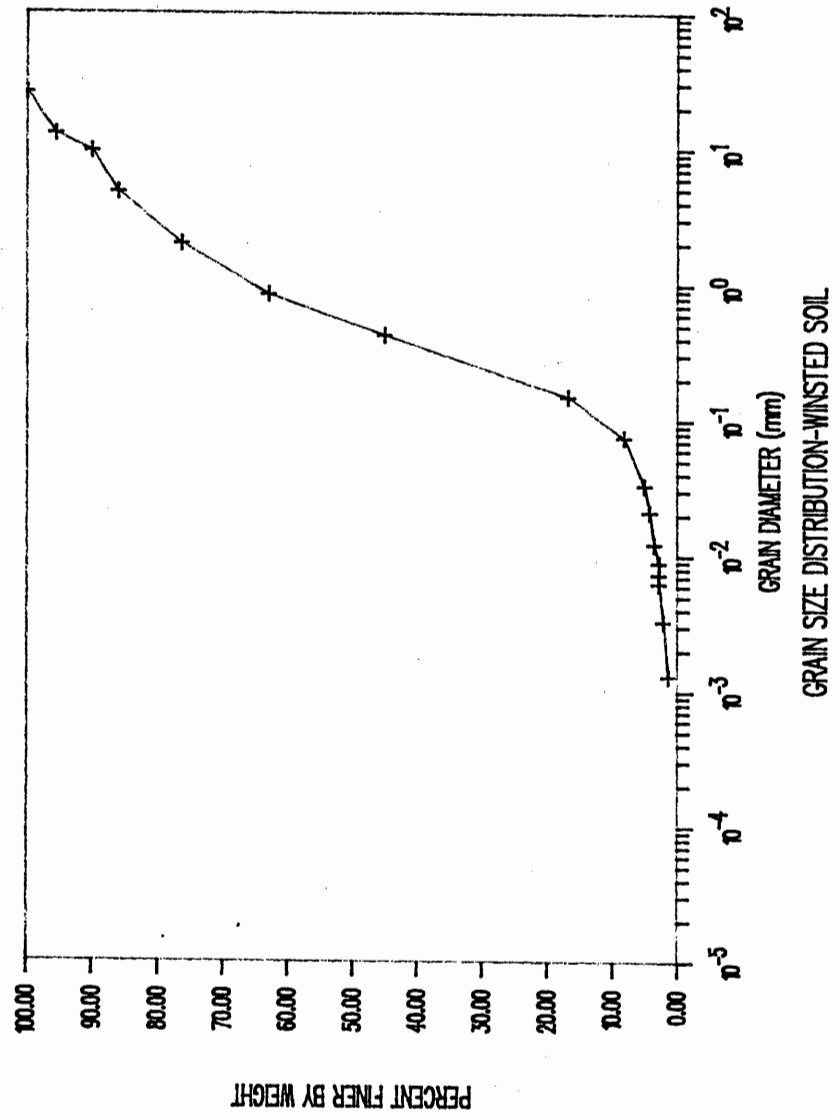
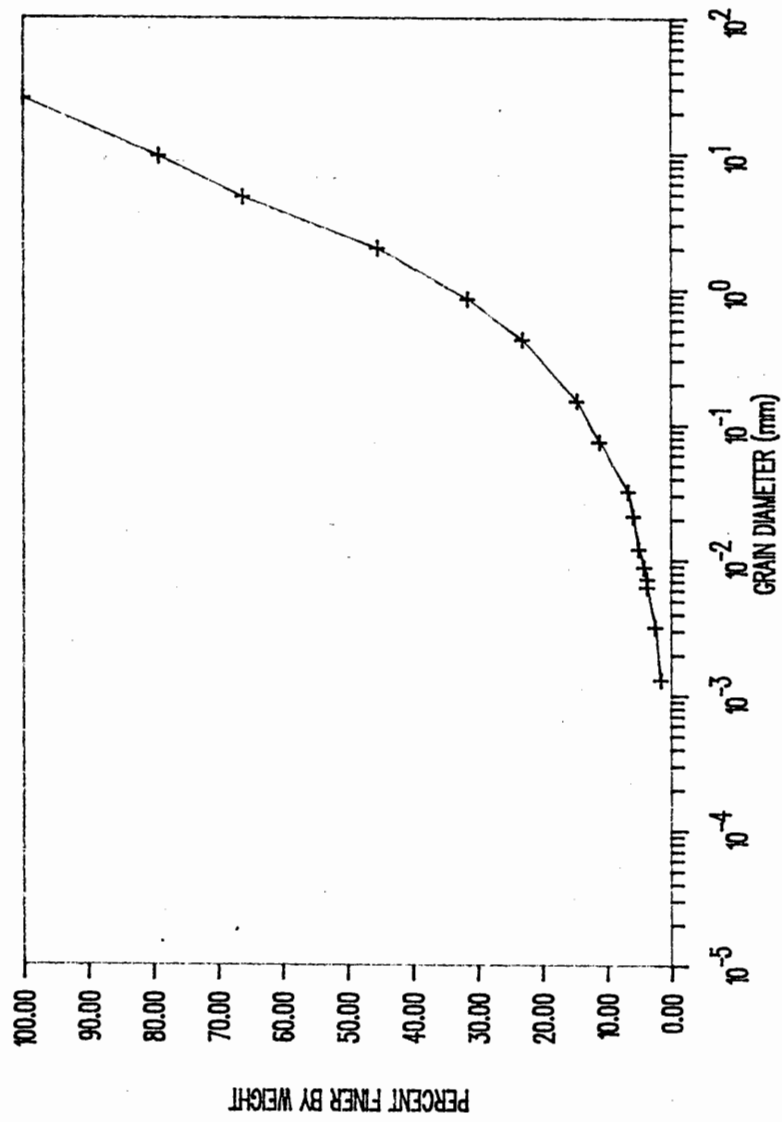


Fig. 5



SIZE DISTRIBUTION OF CONNDOT SOIL

Fig. 6

SOIL SOURCE	% PASSING #10 SIEVE	% PASSING #4 SIEVE	LL	PL	USCS CLASS.	AASHTO CLASS.
MONROE	62	8.8	np	np	SP-SM	A-1-b
WINSTED	75	8.7	np	np	SP-SM	A-1-b
CONNDOT	50	11.2	np	np	SW-SM	A-1-b

TABLE 4 Gradation Characteristics of Soils

#### B. MOISTURE-DENSITY RELATIONS

Compaction tests were performed for each soil in accordance with ASTM Standard D1557-78 Test Method for Moisture-Density Relations of Soils and Soil-Aggregate Mixture. In addition, the minimum and maximum values of the void ratio  $e_{min}$ ,  $e_{max}$ , and the specific gravity of solids,  $G_s$ , were measured and are listed in Table 5. The CONNDOT soil has a higher relative density and specific gravity of solids than the Monroe and Winsted soils.

Figures 7, 8, and 9 show the results of the Standard Proctor Tests. The CONNDOT Processed Soil has a higher maximum dry density than the other soils. This probably results from the higher specific gravity of solids and the gradation off the CONNDOT soil. The CONNDOT Processed Soil is well graded whereas the other soils are uniformly graded. Tighter packing of particles is possible in well-graded soils because a larger variety of particle diameters is available to fill in the spaces between the larger particles.

The relative density of each soil compacted to its maximum dry density was determined based on the evaluations of  $e_{max}$ ,  $e_{min}$ , and  $G_s$  for each soil. The results of this analysis are shown in Table 5.

Evaluation of the relative densities of the Monroe soil samples prepared for resilient modulus testing showed that  $D_R$  was in the range of 95% to 100%. The most probable explanation for this increase is the higher compactive energy per unit volume being applied to the samples prepared for

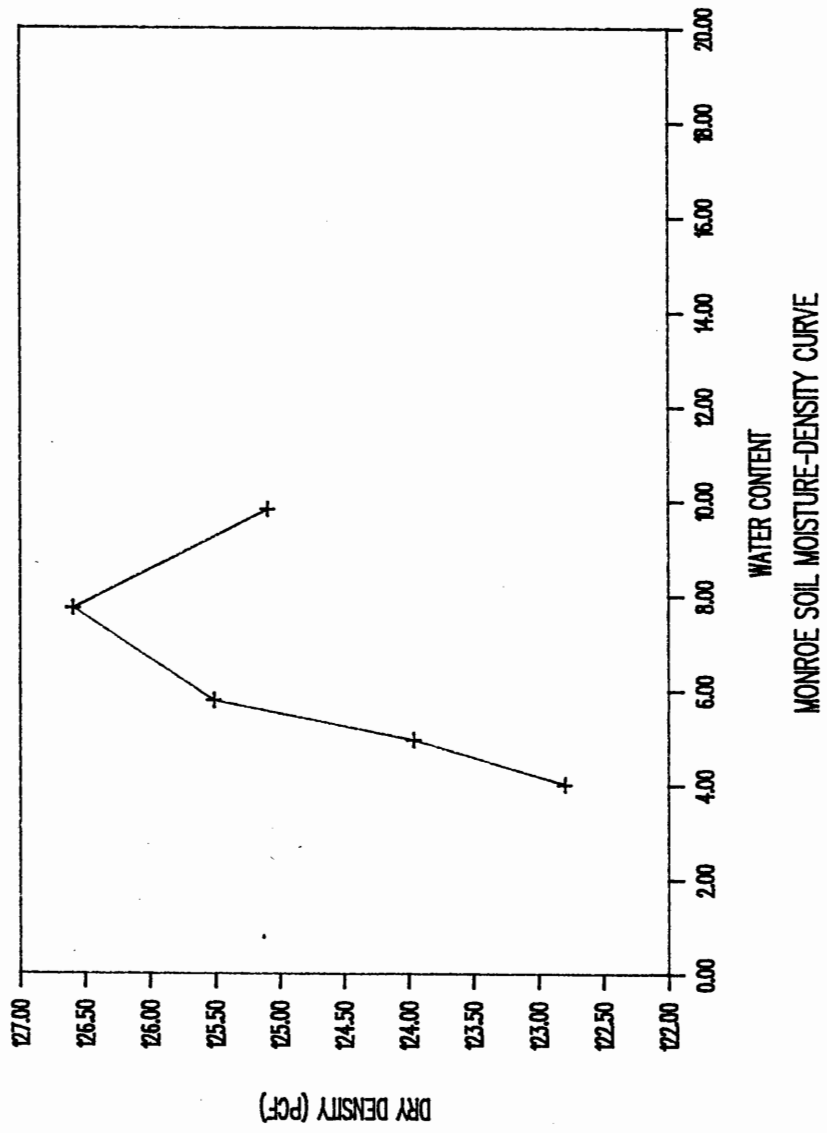


Fig. 7

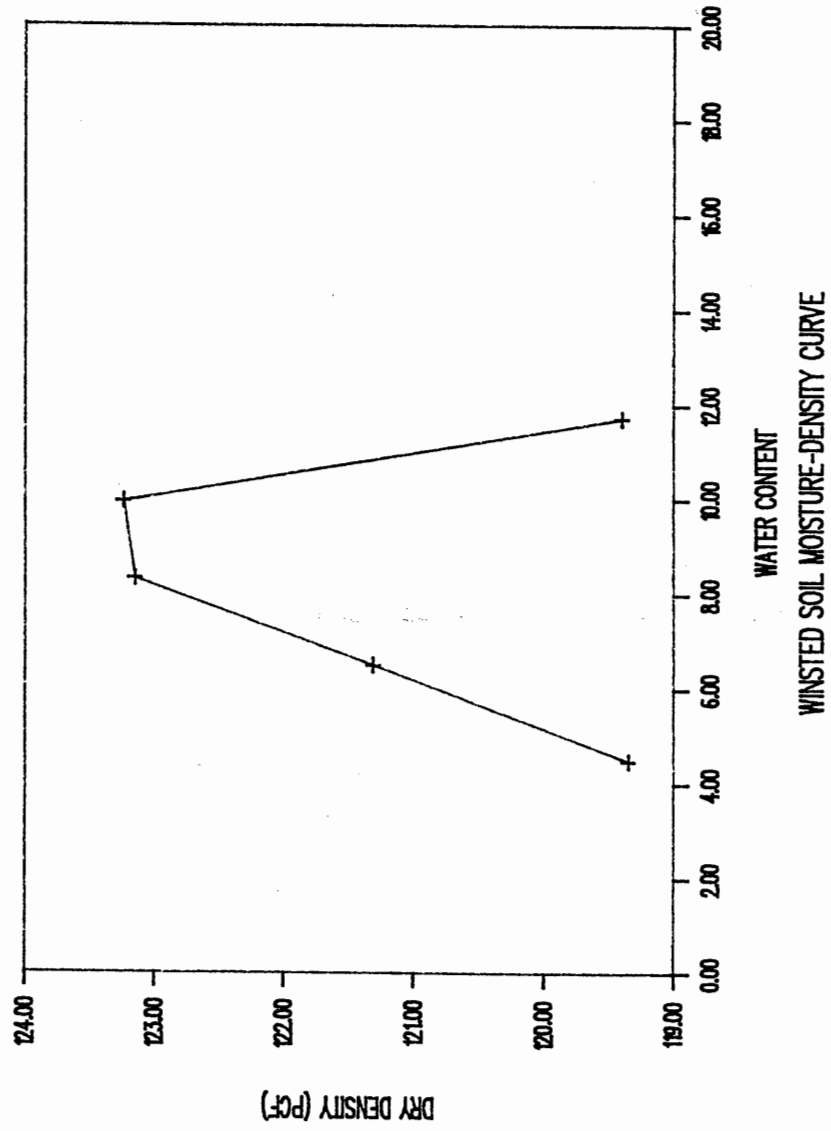


Fig. 8

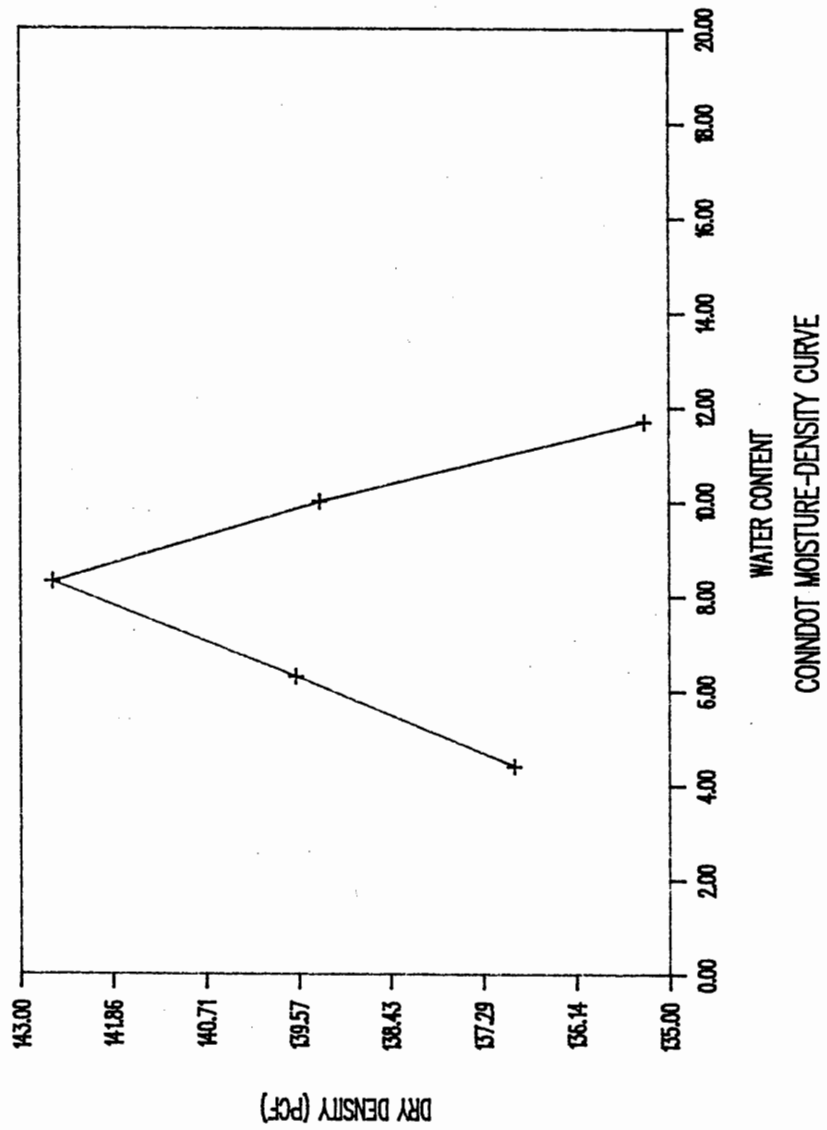


Fig. 9

SOIL SOURCE	MAXIMUM DRY DENSITY	OPT. MOIST CONTENT	Gs	emax	emin	Dr
MONROE	126.5 pcf	7.8%	2.70	0.51	0.26	72%
WINSTED	123.3 pcf	9.0%	2.74	0.78	0.30	82%
CONNDOT	142.5 pcf	8.2%	2.92	0.74	0.27	98%

Table 5 Moisture-Density Properties of Soils

resilient modulus testing than was applied to the moisture-density samples in the compaction test. Tests conducted by Proctor [8] demonstrated that a higher density is achieved with a larger compactive effort.

## VI. TEST EQUIPMENT

The equipment used in the resilient modulus test program can be divided into two categories: equipment required for specimen preparation, and equipment required for resilient modulus testing.

### A. SPECIMEN PREPARATION EQUIPMENT

COMPACTION MOLD - The compaction mold was a modified version of the proctor compaction mold used in the ASTM Standard Test. The modification was an increase of the mold height to eight inches. This modification gave a height to diameter ratio of 2:1, as required for the resilient modulus specimen by AASHTO designation T-274-82 [2].

COMPACTION MACHINE - A Humboldt Model 7300 W Agitate compaction machine was used for sample formation. The machine is equipped with a 10 lb. hammer and set for a fall of 18". The machine is equipped with a counter to set the number of blows desired.

After compaction the specimen was extracted from the mold. A hand-operated hydraulic jack located under the compaction mold at the bottom of the load frame was used to extract the specimen upwards. A steel plate is placed between the sample and the jack to provide a firm reaction surface.

## B. RESILIENT MODULUS TEST EQUIPMENT

TRIAXIAL CELL - A GEOTEST Model S6300 triaxial cell was used to hold the specimen. The chamber was capable of holding a 4" diameter x 8" long sample. To eliminate the frictional forces from the data readings, a load cell was placed inside the chamber. Air was used as the confining fluid to protect the load cell from any detrimental effects, such as electrical short circuits and corrosion, that could result from submersion in water. In addition, the air allows a constant confining pressure as the sample deforms due to the deviator stress.

LOADING SYSTEM - An Instron model 1331 dynamic loading machine was used to apply deviator stresses to the samples. The machine consists of two parts, the control system and the load frame.

The control panel is the device through which load magnitude, duration and pattern are generated and controlled. The system uses a closed-loop control process in which a control module continuously monitors the actual state. If a discrepancy is found between the actual and command states, the control unit drives the system to correct itself (see Fig. 10). This process eliminates the need for the operator to make the necessary adjustments, thus eliminating human error from the load application control process.

The control panel allows the loading system to be controlled by one of three states: load, stroke, or strain. The load control was used in this program because it allowed a direct input of the required deviator stresses.

The load frame consisted of a steel frame with a cross-bar base and a top-mounted actuator. The triaxial cell was mounted to the base of the load cell with two machine screws to secure the cell in position. The hydraulic actuator was the device which applied the required loads to the plunger of the cell. See Fig. 11 for a diagram of the test equipment.

DATA ACQUISITION SYSTEM - The data was collected through an IBM PS2/60 personal computer system. The setup consisted of two linearly variable displacement transducers (LVDTs), one load cell, a Keithley computer interface, and an IBM PS2 computer with the Labtech Notebook data acquisition software.

Two different manufacturers' LVDTs were used in the system: a Transtek model 243-000 and an RDP model D2/200. The Transtek LVDT has a working range of +/- 0.500 inches with an accuracy of +/- 0.003 inches. The RDP LVDT has a working range of +/- 0.200 inches and an accuracy of +/- 0.003 inches. The AASHTO proposed test procedure [12] requires the range of



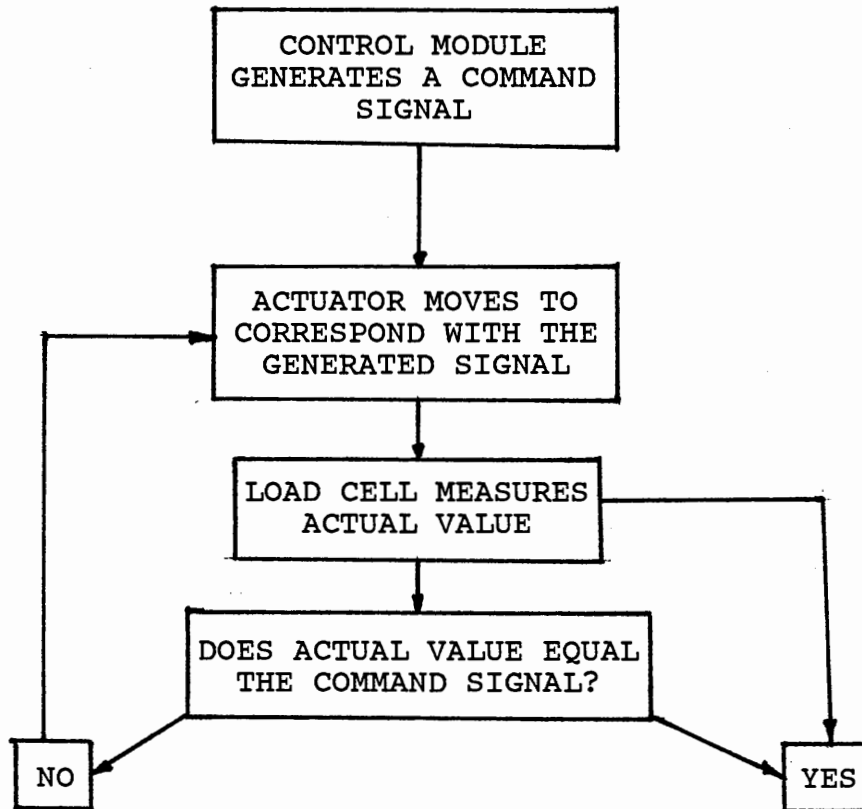


Fig. 10 Flow Diagram for Instron Model 1331 Operation

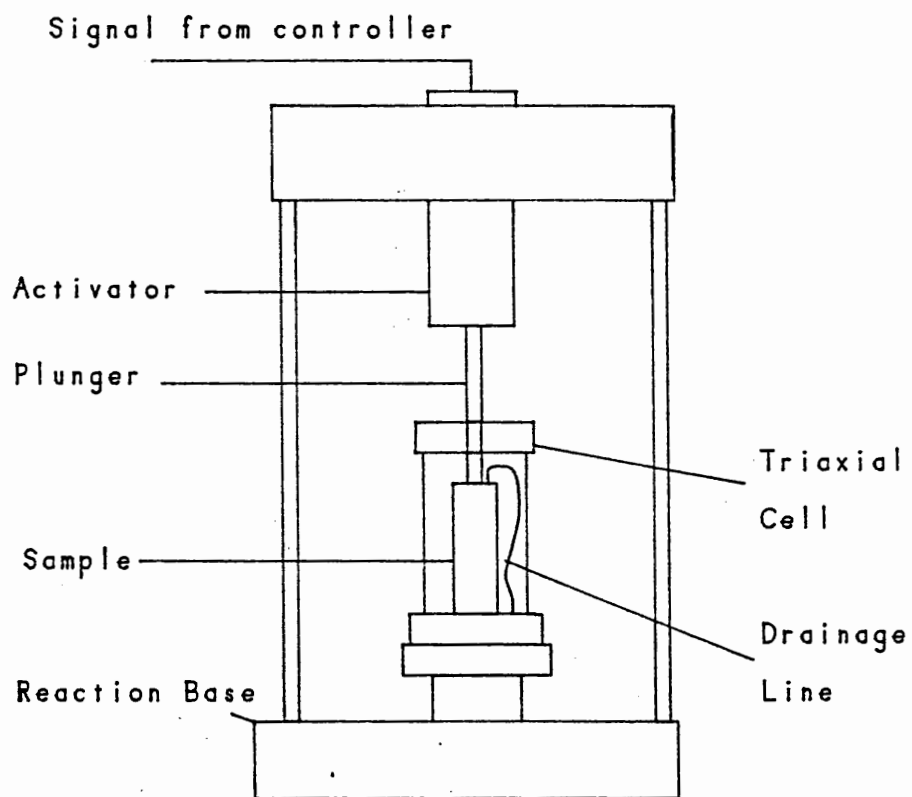


Fig. 11 Instron 1331 Schematic

the LVDTs to be between 0.16 inches and 0.8 inches for an eight inch sample. Both transducers meet this criteria. Since the components qualify under the AASHTO test procedure, no substitutions were made.

The LVDTs were placed on the triaxial cell plunger, rather than clamped directly to the sample. This is due to lack of space within the cell and measuring problems observed by others [11] [12]. Clamping the LVDTs directly to the sample is an unreliable technique. An alternative method of correcting the extraneous equipment strains was developed.

The load cell used is a Wagner Instruments model TH-UM. The load cell has a working range of 0-600 lbs. with an accuracy of +/- 0.73 lbs..

A Keithley Series 500 Hardware Interface was used in the acquisition setup. The system performed the analog to digital conversions of the raw data received from the sensors. The system would then send the converted data to the computer.

The Labtech Notebook software collected the digitized raw data during the test runs. The software was configured so as to convert the raw data into actual forces and displacements. This data was then used in the final analysis.

## C. EQUIPMENT CALIBRATION

### 1. Load Measurement

The data acquisition system was calibrated monthly, as required by the AASHTO proposed test procedure [8].

Calibration was performed by placing a proving ring in place of the soil specimen in the triaxial cell. The load cell was then assembled and equipped with load and displacement sensors. The triaxial cell was placed in the load frame and loaded with a series of predetermined forces. The software was activated at each load to record the raw data. A linear regression was performed on this raw data versus the actual data from the proving ring dial readings. The coefficients determined in the regression analysis were utilized in the software to convert the raw data to actual values. This procedure is in accordance with the approved AASHTO guidelines.

### 2. Strain Tests Using Synthetic Specimen

After installing the transducers and calibrating each one of them independently, the complete system was calibrated.

The calibration procedure consisted of performing the resilient modulus test with a cylindrical specimen made of Urethane Elastomer with known elastic properties. The purpose was to investigate the capability of the system to give reproduceable loading conditions by measuring the resilient modulus of the rubber specimen. The Urethane is considered to be a viscoelastic material with elastic properties independent of the confining pressure, strain amplitude, and stress history but dependent on the loading frequency and the temperature.

The Urethane specimen is a cylinder of 2.8 inches in diameter and 6.85 inches in height. The elastic properties of the specimen as a function of the loading frequency were provided by Professor Kenneth Stokoe, from the University of Texas at Austin. For the specimen used in this project the Resilient Modulus was 8577 psi at a frequency of 25 hz. The AASHTO procedure accepts the use of this synthetic specimen to calibrate the equipment and assure reproduceability of the results [8].

With the specification of the specimen given by Stokoe, et al. [11], the resilient modulus equipment was tested by performing dynamic loading on the rubber specimen. A higher scatter of the data below 10 psi of the principal stress was observed, therefore the data was analyzed at stresses higher than 10 psi using the Least Squares Method.

The resilient modulus values obtained were low due to the deformations recorded by the transducers. Since the transducers were positioned outside the triaxial cell, deformations recorded were higher than those based on the properties of the calibrated specimen. The additional deformations were due to the strain in the system.

The deformation of the apparatus was investigated to correct the total deformation recorded by the transducers. To investigate the deformation of the apparatus, a dynamic test was performed with a steel cylinder. Data obtained from this test showed scatter below a bulk stress of 10 psi due to the inability of the transducers to accurately record deformations smaller than  $4 \times 10^{-6}$  inches. Above 10 psi the scatter was small. The data above 10 psi was used to obtain a correction equation. The deformation obtained from the equation, was subtracted from the deformation recorded by the transducer using the rubber specimen to obtain a corrected deformation reading.

Claros, et al [13] found a 12% difference between the Mr values obtained from the calibration test and the target number specified for the synthetic specimen. They do not

recommend subtracting the deformation of the apparatus from the total deformation because a static solution cannot be applied to a dynamic test. However, performing the subtraction of the load cell deformation, the resilient modulus value for the Urethane specimen was 0.96 % above the value given by the fabricators of the specimen at principal stress higher than 10 psi.

These results predicted an acceptable repeatability of the data to be obtained from the equipment at applied stresses higher than 10 psi. In Resilient Modulus tests, the lowest principal stress  $\sigma_1$  was 8 psi, therefore the scatter of the data was affecting the test in one out of 19 states of stress during the test.

## VII. SPECIMEN PREPARATION AND TEST PROCEDURE

### A. SPECIMEN PREPARATION

The moisture-density relations determined during sample classification were used in the fabrication of each specimen. The maximum dry density and optimum water content were used to calculate the amount of dry soil and water necessary to fabricate the specimen.

The dimensions of each specimen were 4 inches in diameter and 8 inches in length. The specimens were compacted in ten layers. Each layer received 25 blows from a 10 pound hammer falling a distance of 18 inches. The total compactive energy per unit volume of each specimen was 64.4 kip ft/cu. ft, the same as for the AASHTO Modified Proctor Test.

The specimen was then trimmed, as necessary, and extracted from the mold by means of a hydraulic press. Although the soils contained no plastic fines, all specimens were observed to keep their compacted shapes when extracted from the mold. The specimen was immediately weighed, and the degree of saturation estimated.

In the case where the desired saturation was lower than the compacted saturation, the specimen was left exposed to the air to dry. The specimen was periodically weighed until the desired saturation was achieved. The specimen was then sealed in a plastic bag until time for testing.

A second procedure was used when the desired test saturation was higher than the compaction saturation. In this case, the specimen was immediately placed in the triaxial cell and subjected to a hydraulic gradient via the cap and pedestal drainage lines. This procedure forced water into the sample thus increasing the degree of saturation.

Prior to placing the cap on the sample, a mixture of Portland Cement and water was applied to the top of the sample. The purpose of this was to provide an even surface of contact between the sample and the loading cap. Work by Pezo, et al [13], demonstrated that placing grout between the cap and sample provided a full contact surface for load application to the sample. They demonstrated that grouting had a significant effect on the measured resilient modulus and should be included as part of the resilient modulus test procedure.

At the onset of the test program, a leak of the confining air into the specimen was observed. The cause of the problem was determined to be puncturing of the latex membranes by soil particles. A geotextile was placed between the sample and the inner membrane to resolve this problem.

The geotextile acted as a cushion between the soil and membranes, preventing any particles from puncturing the membranes. The geotextile was cut in the vertical direction every one-half inch to allow it to deform without affecting the strain or strength characteristics of the sample. The membranes were secured by two O-rings at both the cap and pedestal.

A test procedure was devised in order to determine if the geotextile was affecting the resilient modulus of the soils tested. Resilient modulus tests were conducted on samples of dry Ottawa sand both with and without the geotextile. Ottawa sand was selected because the particles have no points to puncture the membrane. Analysis of the data showed that the geotextile had no significant effect on the resilient modulus of the sand. It was therefore concluded that the geotextile could be used on the soil samples without altering each soil's measured resilient modulus characteristics.

## B. TEST PROCEDURE

The triaxial cell is assembled and pressure tested for any leakage of the confining fluid through the sample. After the LVDTs were installed, the system was then connected to the data acquisition system and all of the electronic equipment was turned on and allowed to warm up for a period of not less than one hour.

The triaxial cell was placed in the load frame of the Instron and secured to the base plate with bolts. The actuator of the loading machine was lowered until it just touched the plunger of the triaxial cell. All load measuring devices were then zeroed.

The procedure used for testing was the "Proposed Standard Method of Test for Resilient Modulus of Subgrade Soils and Untreated Base/Subbase Materials" [8]. Distinction between granular and cohesive soils was made on the basis of each soil's AASHTO Classification. Inspection of the soil classifications shows all three to be granular.

Testing consisted of a sample conditioning phase followed by the testing program. The purpose of the conditioning phase is to insure that a good contact is established between the soil and the cap. The resilient modulus of the sample was monitored during the test segment.

The load signal consisted of a haversine wave where the load duration was 0.4 seconds and the relaxation period 0.9 seconds. Data was collected for the last five load cycles of each load combination of deviator and confining stress. Data was collected at a rate of 30 Hz via the Labtech Notebook Software.

The load combinations used in the test procedure were for granular samples of base/subbase materials. Table 6 is a summary of the testing program for each specimen.

LOAD CASE	CONFINING STRESS	DEVIATOR STRESS	NUMBER OF REPETITIONS	PHASE
1	20	15	200	CONDITIONING
2	20	10	50	TESTING
3	20	20	50	
4	20	30	50	
5	20	40	50	
6	15	10	50	
7	15	20	50	
8	15	30	50	
9	15	40	50	
10	10	5	50	
11	10	10	50	
12	10	20	50	
13	10	30	50	
14	5	5	50	
15	5	10	50	
16	5	15	50	
17	3	5	50	
18	3	7	50	
19	3	9	50	

Table 6 Test Sequence for Granular Specimens  
Base/Subbase Material

After completion of the test sequence, the specimen was removed from the chamber. Two water content samples were taken from the center of the sample to measure the water content and determine the degree of saturation.

The test program investigated two aspects of the effect of water content on the resilient response of the soil. First, the Monroe soil was compacted at optimum water content, then the degree of saturation was varied in order to determine the variation of the resilient modulus with saturation.

All three soils were run in a series of tests which measured the resilient modulus of samples which were either free draining or undrained. The intent was to investigate how the resilient modulus changes based on drainage characteristics of the roadway system.

A third series of tests investigated the effect of water content at compaction on the resilient response of the CONNDOT and Winsted soils. Samples of each soil prepared wet, dry, and at the optimum water content were tested to determine their resilient characteristics. The purpose of this procedure was to determine the effects of compaction water on the resilient modulus.

## VIII. DATA ANALYSIS AND RESULTS

### A. GENERAL

The effects of moisture, drainage, and compaction water content on the resilient modulus of soils were investigated. Tests on the three Connecticut soils investigated the resilient response of each soil under conditions where pore pressures were both allowed and prevented from dissipating. In addition, the effects of varying the compaction water content by +/- two percent of the optimum moisture content was investigated. The Monroe soil was tested to determine the variation in the resilient modulus of that soil with percent saturation.

Before proceeding with the data analysis, a discussion of two soil parameters which are involved in the analyses is warranted. The parameters are percent saturation and pore pressure.

The percent saturation of a soil is a volumetric relation. The total volume of a soil mass is the sum of three volumes: the volume of solids, volume of water, and the volume of air. The volumes of water and air can be combined into the volume of voids. The percent saturation is the ratio of the volume of water to the volume of voids. A soil at 100%



saturation has a void space which is completely filled with water, whereas a soil at 0% saturation has no water in its void space.

The stress applied to a soil is called the total stress. The total stress consists of two components, the effective stress and the pore pressure. The effective stress is that portion of the total stress which is passed through inter-particle contacts. The pore pressure is the portion of the total stress which is carried through the pore fluids. The total stress and the pore pressure can both be measured, whereas the effective stress must be calculated from these measured values. The effective stress is a representative value of the inter-particle stresses averaged across the entire cross-section of the soil mass. The stresses at the particle contacts are actually much larger than this average value. In a triaxial cell, the confining stress is the total stress on the sample.

#### B. PERCENT SATURATION AND THE RESILIENT MODULUS

Recall from Section II that the equations used to evaluate the resilient modulus are:

$$M_r = K_1(\sigma_c)^{K_2} \quad 2$$

$$M_r = K_1'(\theta)^{K_2'} \quad 3$$

where

$\sigma_c$  = confining stress

$\theta$  = bulk stress ( $\sigma_1 + \sigma_2 + \sigma_3$ )

$K_1, K_2, K_1', K_2'$  = regression coefficients

All regression analyses were performed using the Quattro, a spreadsheet software. Equations 2 and 3 were converted to a linear format by expressing the equations in logarithmic form.

Table 7 lists the regression coefficients for  $M_r$  as a function of confining stress for samples of Monroe soil at various degrees of saturation. The parameters  $K_2$  and  $K_2'$  in Table 7 are the slopes of the regression lines. A trend of decreasing slope with decreasing saturation is observed from results. A rather sharp increase in slope is observed at a percent saturation higher than 81%.

Figure 12 presents the data in Table 7 in graphical form. A considerable amount of scatter is noted for the case of saturation equal to 89%. A possible explanation for this is that there are two separate regression lines for this data.

SATURATION	K1 (psi)	K2	r <sup>2</sup>
89%	2186	0.70	0.87
81%	6236	0.49	0.99
42%	11746	0.39	0.97
17%	20771	0.38	0.98

Table 7 Regression Coefficients for Monroe Soil as a Function of Confining Stress at Various Degrees of Saturation

A steeper line could represent the data above 10 psi confining stress, while a flatter slope could represent the data below 10 psi. A possible mechanism through which this might occur is the following: Testing begins at the highest confining stress, which causes a considerable amount of water to exit the sample. Little, if any, capillarity exists in the sample at these higher confining stresses. The sample has a tendency to swell as the confining stress is lowered. Negative pore pressures (capillary forces) develop as a result of the swelling. These capillary forces are tensile forces which pull the individual particles together. The net result is a sample experiencing an effective confining stress which is larger than the chamber confining pressure. This implies that the sample is stiffer than the external confining stress would indicate.

The slope of the curve with no capillarity is considerably larger than the recommended value found in the AASHTO proposed design guide [10]. The slope calculated for the Monroe soil is 0.9 whereas the value suggested by AASHTO is 0.7. It is noted that AASHTO's recommended value matches the value determined for the test listed in Table 7. The AASHTO recommended value is most likely a conservative value and may represent a best-fit to data which is not truly linear in nature.

A second observation noted in Fig. 12 is the trend of increasing resilient modulus with decreasing saturation. This indicates that increasing the amount of water in the sample has a softening effect on the soil. This is attributed to capillary tension at the lower percent saturations. Thus the soil is at a higher effective confining stress.

The regression coefficients for the resilient modulus as a function of bulk stress for the Monroe soil are given in Table 8.

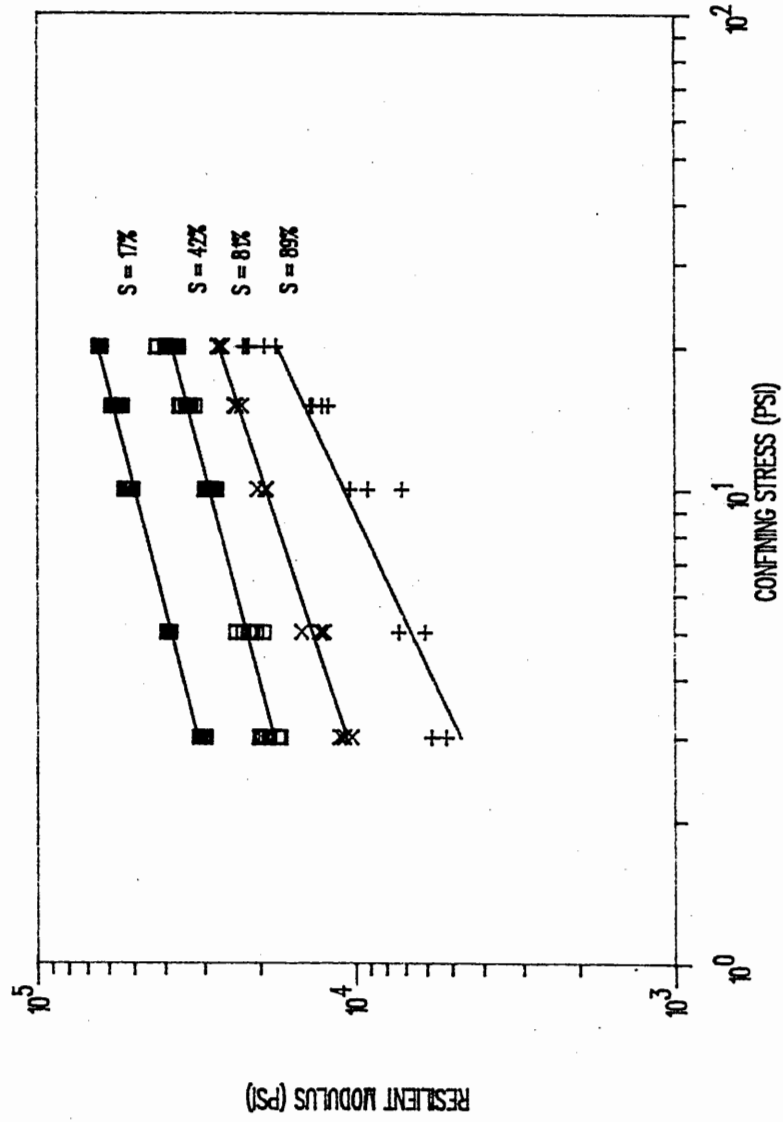


Fig. 12 Resilient Modulus vs. Confining Stress for the Monroe Soil @ Various Percent Saturations

SATURATION	K1' (psi)	K2'	r <sup>2</sup>
89%	513	0.79	0.82
81%	2574	0.52	0.95
42%	5796	0.42	0.89
17%	10586	0.40	0.89

Table 8 Regression Coefficients for Monroe Soil as a Function of Bulk Stress

Again, the same trends of decreasing slope with decreasing percent saturation are observed. Comparisons of the correlation coefficients,  $r^2$ , listed in Tables 7 and 8 indicate that modeling the resilient modulus as a function of confining stress is a better correlation than the resilient modulus as a function of bulk stress.

Figure 13 is a graphical representation of the data in Table 8. Noted again is the trend of decreasing resilient modulus with increasing saturation. In addition, the slopes of the lines flatten as the saturation decreases, similar to those as a function of confining stress. Greater scatter, as indicated by the correlation coefficients, is apparent in this figure.

### C. DRAINAGE CONDITIONS AND THE RESILIENT MODULUS

Tests were conducted on specimens of all three soils in the drained and undrained states. The specimens were compacted at the optimum water content and tested with the drain valves on triaxial cell open, and then retested with the drain valves closed. The drain valves were opened when switching confining pressures to allow excess pore pressures to dissipate. Data analysis again investigated the resilient modulus as function of confining and bulk stress.

Table 9 lists the regression coefficients for resilient modulus versus confining stress and bulk stress for the three soils.

Figures 14 and 15 are graphs of the drained and undrained regression lines for the Monroe soil. The undrained resilient modulus is less than the drained resilient modulus in both

SOIL TYPE	SAT %	K1(psi)	K2	R <sup>2</sup>	K1'(psi)	K2'	R <sup>2</sup>
MONROE	75	4941	0.55	0.93	1941	0.57	0.87
MONROE	81	5042	0.56	0.98	1940	0.58	0.93
MONROE	87	1424	0.91	0.88	226	1.03	0.90
WINSTED	73	4259	0.52	0.97	1879	0.53	0.83
WINSTED	79	7011	0.45	0.96	3132	0.48	0.89
CONNDOT	80	6139	0.52	0.88	2701	0.53	0.75

Table 9 Regression Coefficients for Drained and Undrained Conditions as a Function of Bulk Stress and Confining Stress

cases. Statistical analyses show a significant difference between the drained and undrained states for both cases. The difference is greater for a degree of saturation of 75% than for 81%. During testing of the specimen having a degree of saturation equal to 81%, it was noticed that water was drawn into the sample when the drain valve was opened during confining stress changes. This observation would indicate negative pore pressures and, thus, inter-particle tension existing in the sample. This could be an explanation of an  $M_r$  which is higher for 81% saturation than for 75% saturation.

Figure 16 is a graph of the three undrained cases for the Monroe soil. The figure depicts that the slope of the regression line is relatively constant for the cases of 75% and 81% saturation. Above 81% saturation, the slope increases sharply. The scatter of the data,  $r^2 = 0.88$ , for the sample at 87% saturation indicates that the data may represent two regression lines, as discussed previously for this soil. The slope would be steeper at high confining stresses and flatten out due to capillary tension at lower pressures. This is the same trend discussed in the previous section.

Figures 17 and 18 are plots of the regression lines showing the results for the drained and undrained tests for the Winsted soil. Notice at 73% saturation the resilient modulus for the drained state is greater than for the undrained case. When the saturation increases to 79%, however, the undrained case shows a higher resilient modulus than the drained case. Statistical analyses show no significant difference between the drained and undrained states for both cases. The drained and undrained cases are, therefore, considered to be the same with regards to the resilient properties of the soil.

Negative pore pressures were present during testing of the specimen at 79% saturation. The presence of this

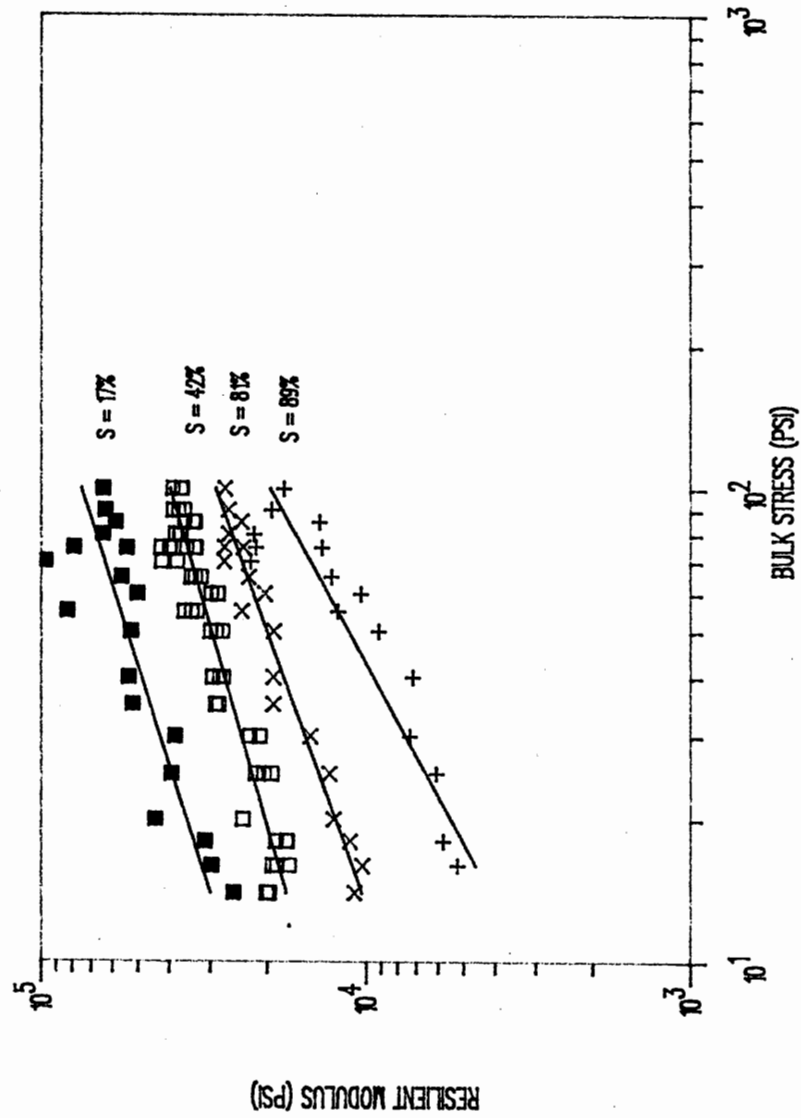


Fig. 13 Resilient Modulus vs. Bulk Stress for the Monroe Soil at Various Degrees of Saturation

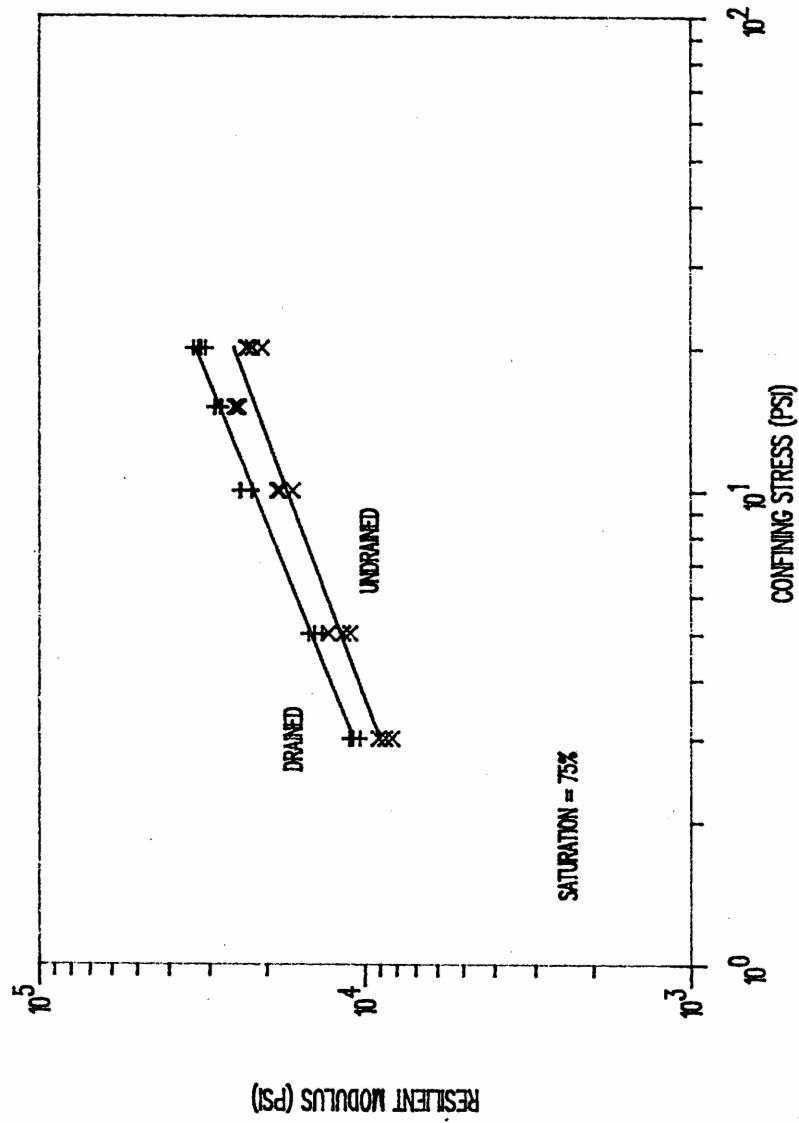


Fig. 14 Resilient Modulus vs. Confining Stress for the Monroe Soil in the Drained and Undrained States

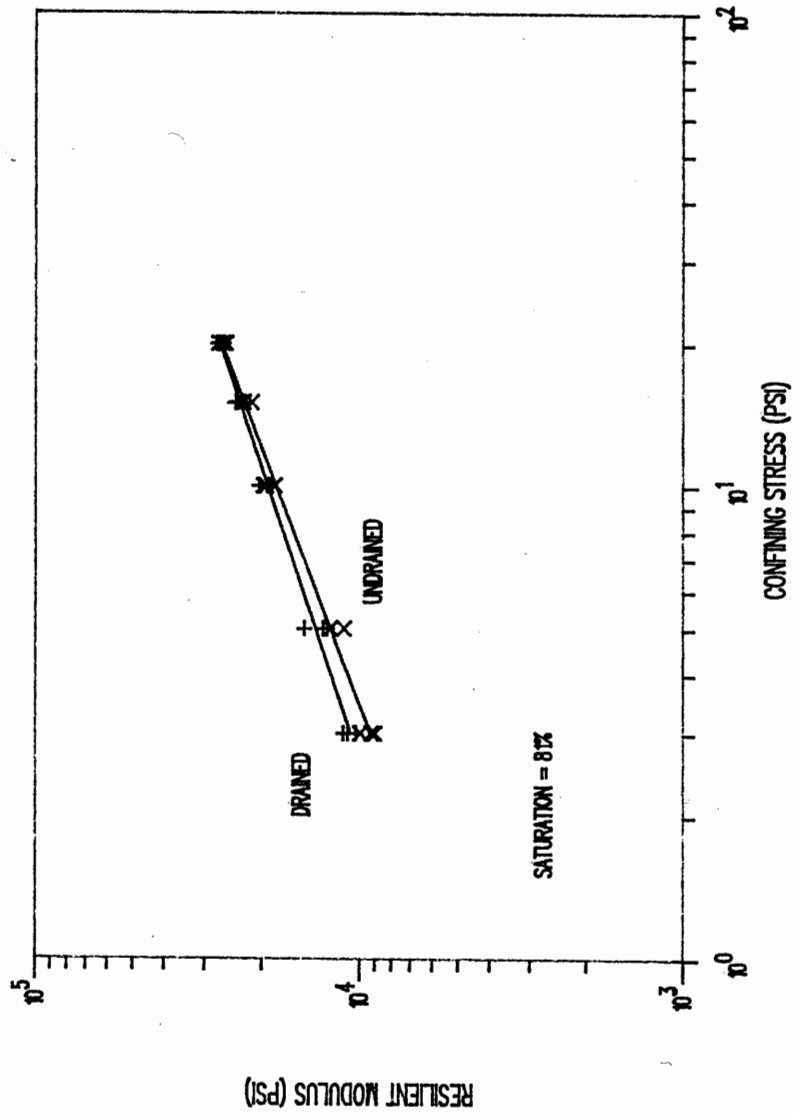


Fig. 15 Resilient Modulus vs. Confining Stress for the Monroe Soil in the Drained and Undrained States



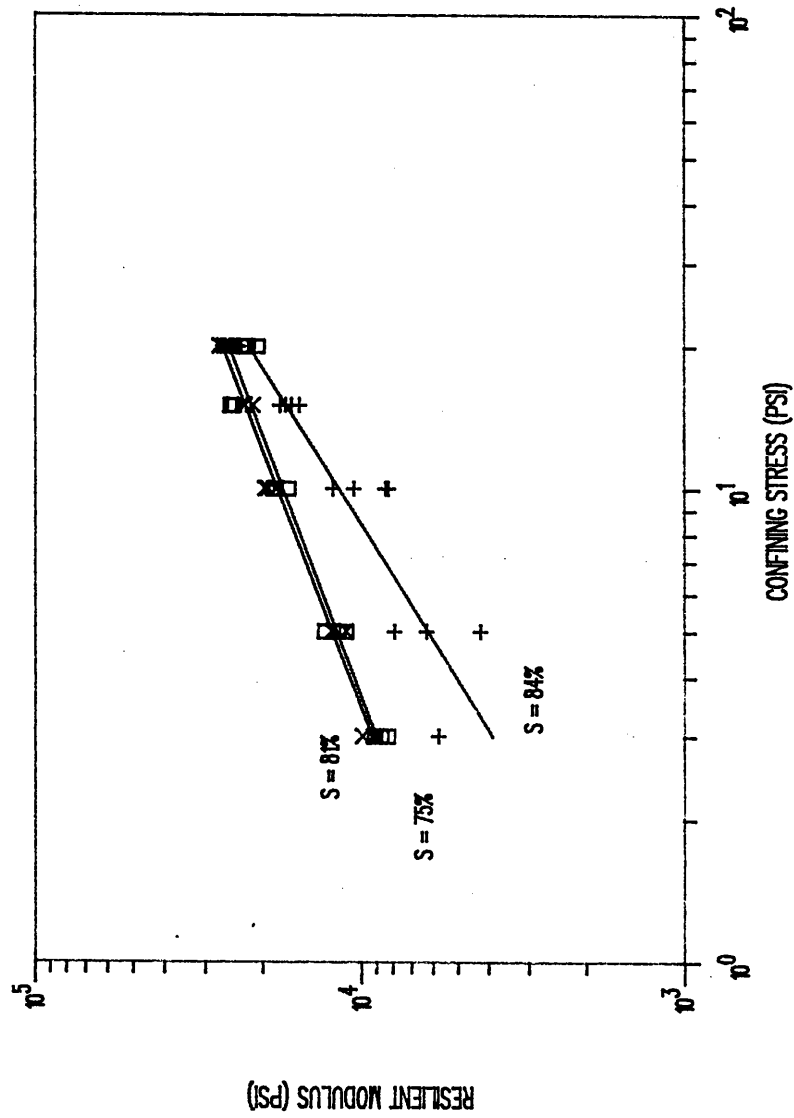


Fig. 16 Undrained Resilient Modulus vs. Confining Stress for the Monroe Soil at Various % Saturations

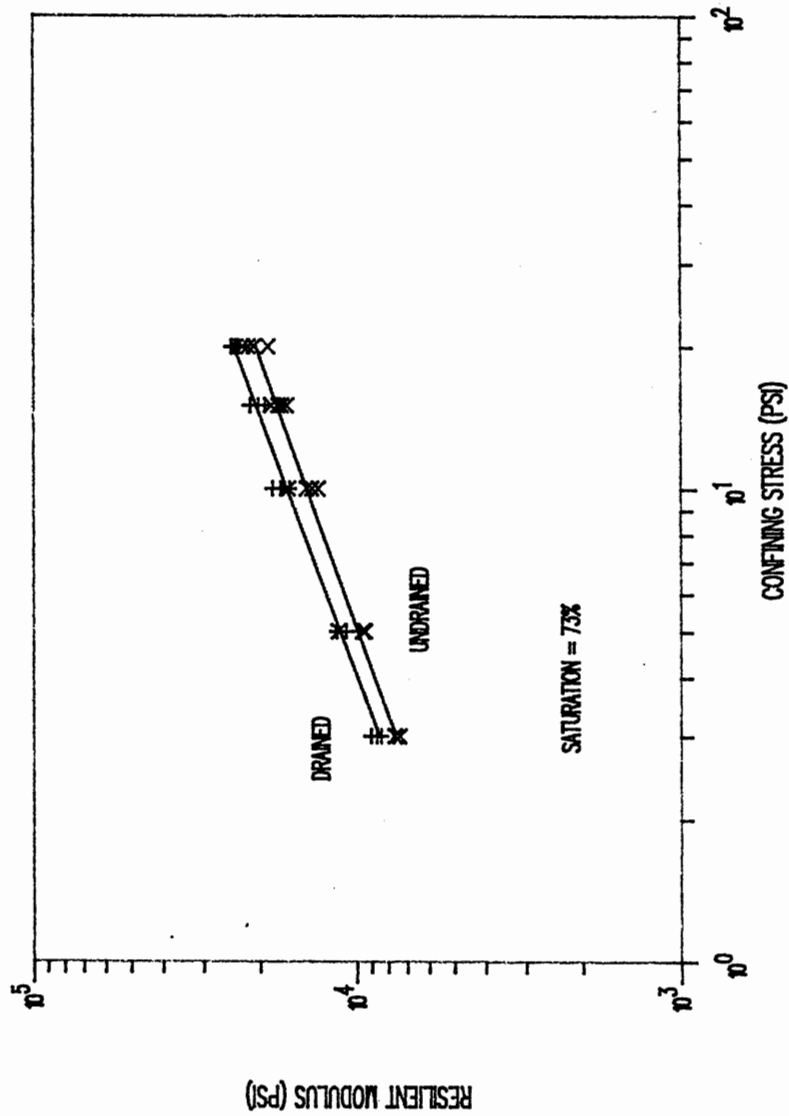


Fig. 17 Resilient Modulus vs. Confining Stress for the Winsted Soil in the Drained and Undrained States

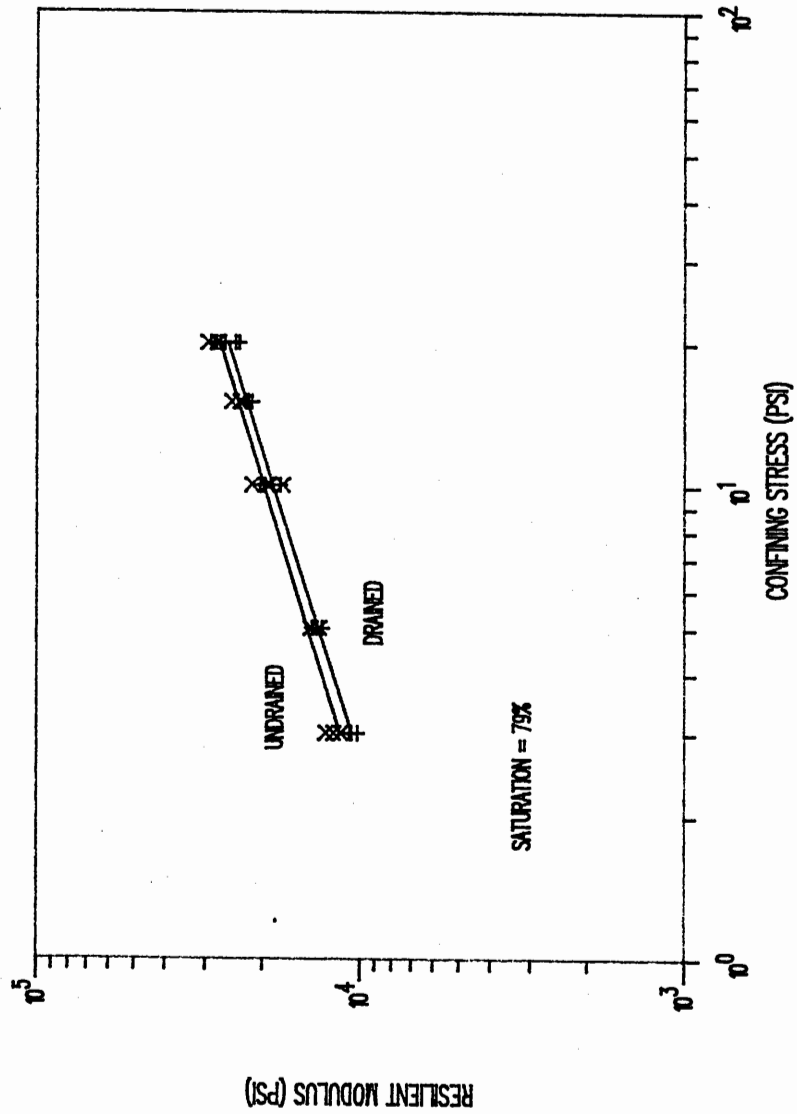


Fig. 18 Resilient Modulus vs. Confining Stress for the Winsted Soil in the Drained and Undrained States

condition is based on the observation of water being drawn into the sample during the test. This may account for the increase in the resilient modulus in the undrained state. Negative pore pressures were not observed during the testing of the sample at 73% saturation. The void ratios of the samples were identical at 0.32.

Figure 19 shows the resilient modulus vs confining stress for the drained and undrained cases of the CONNDOT soil. Statistically, no significant difference exists between the slopes of the two lines at the 90% confidence level. Therefore, there is no difference between the drained and undrained states. Negative pore pressures were observed during these test procedures.

The most enlightening information concerning the effects of drainage on the resilient modulus are from a test procedure devised for the Monroe soil. Two specimens were fabricated using the optimum moisture content for compaction purposes. After placing each specimen in the cell, water was allowed to enter each specimen through the base. This made each sample's degree saturation increase to greater than 85%.

One specimen was tested with the drain valves open, whereas the other specimen was tested with the drain valves closed from the start of testing. The results are shown in Figure 20. A regression line was calculated for the undrained case but the  $K_2$  value was negative, indicating too much scatter. This figure depicts the drastic reduction in resilient modulus resulting from the inability of excess pore pressures to dissipate.

#### D. COMPACTION WATER CONTENT AND THE RESILIENT MODULUS

In order to properly apply the resilient modulus of soils to pavement design, it is necessary to understand the parameters which may alter the resilient characteristics of a soil. One area of interest is the effect of placement conditions on the resilient modulus. Specifically, the variation of compaction water content has been investigated to determine its effect on the resilient behavior of the Winsted and CONNDOT soils.

Table 10 lists the regression coefficients for the resilient modulus as a function of confining stress for Winsted and CONNDOT samples compacted under various moisture conditions. Specifically, the effect of compacting each soil two percent wet and dry of optimum was investigated.

Figures 21 and 22 are graphical representations of the data in Table 10. Figure 21 shows a reduction in resilient

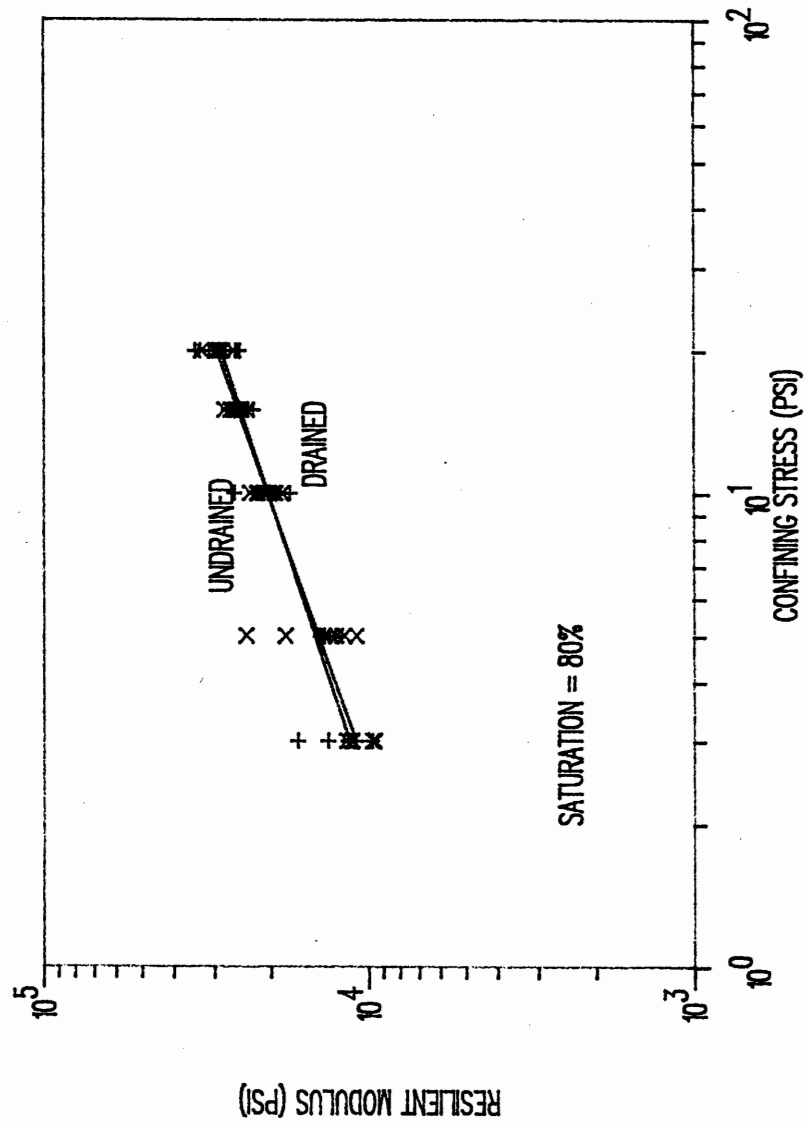


Fig. 19 Resilient Modulus vs. Confining Stress for the CONNDOT Soil in the Drained and Undrained States

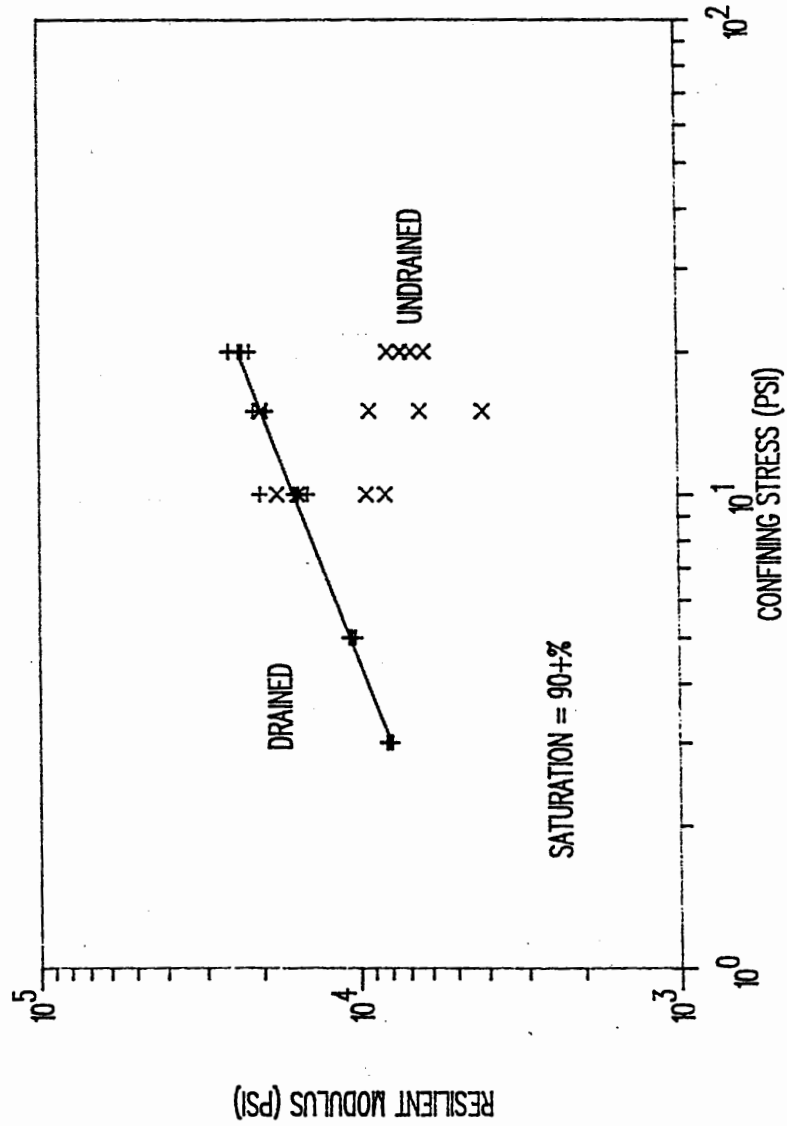


Fig. 20 Drained vs. Undrained Resilient Moduli for Monroe Soil

SOIL TYPE	Water Content Relative to omc	K1(psi)	K2	Dr %
WINSTED	omc	5954	0.48	95
WINSTED	dry	5882	0.52	102
WINSTED	wet	5614	0.47	88
CONNDOT	omc	6728	0.48	102
CONNDOT	dry	5081	0.60	106
CONNDOT	wet	6274	0.47	97

Table 10 Regression Coefficients for Various Compaction Water Contents

modulus as the water content at compaction increases. This trend is attributed to two factors: a decreasing relative density with increasing compaction water content, and a decreasing soil strength with increasing saturation.

This information does not indicate that the soil should be compacted dry of optimum, as the figure would seem to indicate. It must be remembered, as pointed out in Section VII A, that the compactive energy per unit volume is higher for the samples than it is for the Proctor moisture-density tests. Increased compactive energy translates to decreased optimum moisture content, as indicated by Proctor [14].

Figure 22 corresponds to the data for the CONNDOT soil. A definite decrease in resilient modulus is observed moving from the optimum water content to wet of optimum. The sample compacted dry of the optimum moisture content has a measured resilient modulus regression line with a steeper slope than the other two samples.

#### IX. SUMMARY AND CONCLUSIONS

The following observations were made concerning the resilient moduli of the three Connecticut soils.

A trend of decreasing resilient modulus with increasing moisture content is observed in the data for the Monroe soil. The resilient modulus at 1 psi confining stress is 10,586 psi at 17% saturation but only 513 psi at 89% saturation.

An 80% reduction is observed in the resilient modulus when the degree of saturation increases from 81 to 89%. This seems to indicate that there is a critical degree of

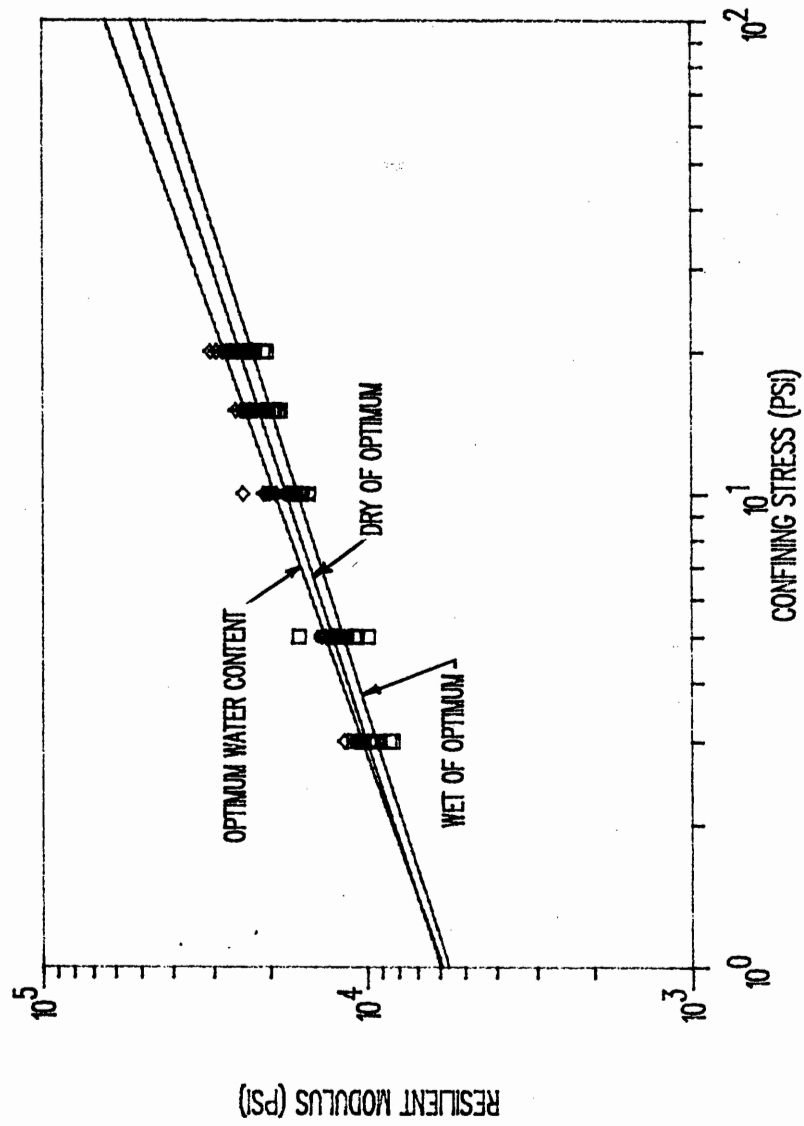


Fig. 21 Effect of Varied Compaction Water Contents on the Resilient Modulus of Winsted Soil



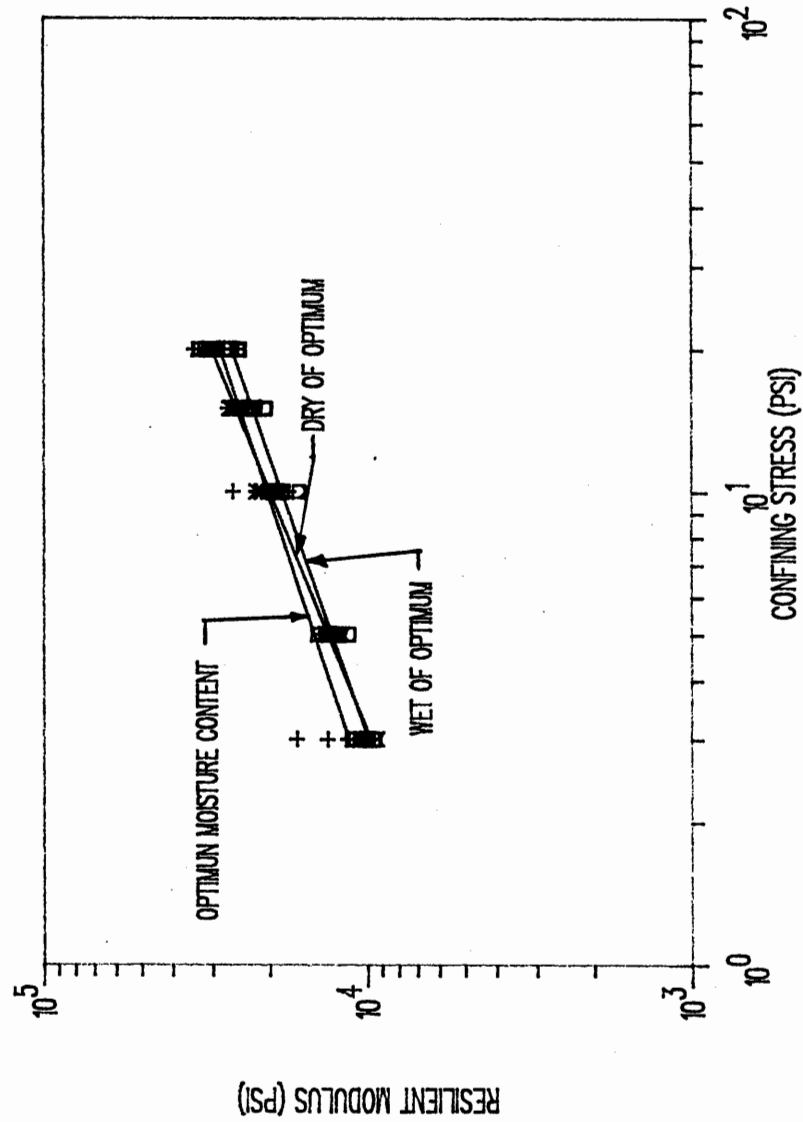


Figure 22 Effect of Varied Compaction Water Contents on the Resilient Modulus of CONNDOT Soil

saturation located between these two values, where the resilient characteristics of the soil become unstable, thus dramatically reducing the load-carrying capabilities of the soil.

The resilient modulus as a function of confining stress was found to yield a higher correlation coefficient than does the resilient modulus as a function of bulk stress. This fact indicates that the resilient modulus as a function of confining stress is the more accurate of the two models for representing the soils studied in this program.

Tests were performed to compare the drained and undrained resilient moduli of the Monroe, Winsted, and CONNDOT soils. The results show minor differences between the two cases. It is believed that capillary forces assume some role in the undrained state. For a given soil, this effect may be dependent on the saturation below which no positive pore pressures can develop.

The Monroe soil shows a decrease in resilient modulus when the sample is undrained as compared to drained. An observation of water being drawn into the sample was made during one test run. This sample (saturation = 81%) shows a smaller difference between the drained and undrained resilient moduli than does the sample at 75% saturation. It is believed that capillary forces are stiffening the sample and thus increasing the resilient modulus in the undrained state.

The Winsted soil shows a decrease in resilient modulus in one instance, but an increase in the other, when going from the drained to the undrained state. Again, water was observed being drawn into the sample which had a resilient modulus higher in the undrained than drained state. Dilatation of the soil skeleton is the cause of the development of the capillary forces. These capillary forces are suspected of increasing the resilient modulus to a value greater than what the soil skeleton alone would yield.

The CONNDOT soil yields the same resilient modulus for the drained and undrained states. No significant difference was found between the two states for both samples. Negative pore pressures (i.e., water being drawn into the sample) were observed in both cases.

A second test procedure investigated the drained and undrained resilient moduli where the undrained state allows no excess pore pressure to dissipate. This test was performed on samples at least 7% above the saturation of the Monroe soil sample after compaction. The results show a dramatic reduction in resilient modulus from the drained to undrained state. In fact, the sample failed during undrained testing.

These results illustrate two important points. First, the resilient modulus of a granular soil will be high if the sample is allowed to properly drain. Second, proper evaluation of the drainage conditions is necessary to test the soil properly.

The Winsted and CONNDOT soils were tested to determine the variation of resilient modulus with compaction water content. The Winsted soil shows a decreasing resilient modulus with increasing compaction water content. This is the effect of increasing dry density and decreasing soil stability with increasing water content.

The results for the CONNDOT soil show a decrease in resilient modulus moving from the optimum moisture content to wet of this value.

## REFERENCES

1. NCHRP "Proposed AASHTO Guide for Design of Pavement Structures," NCHRP Project 20-7/24 PPAA-1-AA51, 1984.
2. "Standard Method of Test for Resilient Modulus of Subgrade Soils," AASHTO Designation T274-82, 1986.
3. Hveem, F.N., "Pavement Deflections and Fatigue Failures," HRB Bulletin 114, pp 43-73, 1955.
4. Seed, H.B., Mitry, F.G., Monismith, C.L., Chan, C.K., "Prediction of Flexible Pavement Deflections from Laboratory Repeated-Load Tests," NCHRP R35, pp 3-47, 1967.
5. Elliott, R.P., Thornton, S.I., "Simplification of Subgrade Resilient Modulus Testing," Transportation Research Record 1192, TRR National Research Council, Washington, DC, pp 1-7, 1988.
6. Wilson, B.E., Sargand, S.M., Hazen, G.A., Green, R., "Multiaxial Testing of Subgrades," Transportation Research Record 1278, TRR National Research Council, Washington, DC, pp 91-95, 1990.
7. Hicks, R.G., "Factors Influencing the Resilient Response of Granular Materials," HRB 345, pp 15-31, 1971.
8. "Proposed Standard Method for Resilient Modulus of Subgrade Soils and Untreated Base/Subbase Materials," AASHTO Subcommittee on Materials, 1990, pp 1-35.
9. Rada, G., Witczak, M.W., "Comprehensive Evaluation of Laboratory Resilient Moduli Results for Granular Material," Transportation Research Record 810, TRR National Research Council, Washington, DC, pp 23-32, 1981.
10. "Proposed AASHTO Guide for Design of Pavement Structures," NCHRP Project 20-7/24, 1985.
11. Claros, G., Hudson, W.R., Stokoe, K.H. II, "Modifications to Resilient Modulus Testing Procedure and Use of Synthetic Samples for Equipment Calibration," Transportation Research Record 1278, TRR National Research Council, Washington, DC, pp 51-62 (1990).

12. Stohe, K.H. II, Kim, D. and Andrus, D., "Development of Synthetic Specimens for Calibration and Evaluation of Resilient Modulus Equipment," Transportation Research Record 1278 TRR, National Research Council, Washington, DC, pp 63-71 (1990).
13. Pezo, R.F., Claros, G., Hudson, W.R., "An Efficient Resilient Modulus Testing Procedure for Subgrade and Non-Granular Subbase Materials," (Preprint), Transportation Research Board, pp 1-26, 1992.
14. Holtz, R.D., Kovacs, W.D., An Introduction to Geotechnical Engineering, Prentice-Hall, Inc., New Jersey, pp 111-112, 1981.